Joint Defra/EA Flood and Coastal Erosion Risk Management R&D Programme

Development of estuary morphological models

Annex F: Intercomparison of models predicting estuarine morphology

R&D Project Record FD2107/PR



Environment Agency

defra
Department for Environment Food and Rural Affairs

Intercomparison of models predicting estuarine morphology

Executive Summary
Models are needed to predict changes in estuaries over many decades, for management and to assess future flood risk. This challenge for estuarine morphology studies is the subject of the Defra/Environment Agency UK Estuaries Research Programme and the component project FD2107 *Development of estuary morphological models*.

In FD2107, seven models of varied approach ("bottom-up", "top-down", "Hybrid" and inverse) have been compared in UK estuaries. Responses to possible scenarios 50 years hence were considered: changed river flow, tidal range, mean and surge levels and wave stresses. The estuaries were the Thames, Blackwater, Humber, Mersey, Dee, Ribble, Southampton Water, Tamar.

Of the models applied to the Thames, only ASMITA suggested that Thames infill keeps up with sea-level rise, in accord with the findings of Historical Trend Analysis.

The Emulator struggles to represent intertidal areas consistent with high and low water areas. It cannot model loss of intertidal areas or constraints on high-water area by fixed structures.

A Hybrid Regime model, and models with particle tracking in 2D and 3D, can represent low-water and high-water areas and volumes, limited only by the chosen resolution. The particle-tracking models predict sediment transport and deposition but suffer from having to continually repeat flow model runs as bathymetry evolves.

These models (especially the Hybrid Regime model) and ASMITA can represent constraints on high water area and hence "coastal squeeze" as mean sea level rises. Otherwise, ASMITA loses intertidal area only if sea level rise accelerates and infill lags behind.

Historical trend analysis can guide expectations of future trends if applied within the range of experience. An Inverse model also uses previous changes, with more reference to dynamics via a bed-evolution equation. Predictions depend on relatively frequent surveys.

Some areas of scope for future development of models are suggested.

If data are lacking for validation against historic change, then generation of an ensemble of possible outcomes is recommended, to test model results against alternatives and validate predicted future morphologies.

Estuaries do not all respond in the same way. This puts an onus on modelling the particular estuary studied.

Contents

1. Introduction

Interest in estuaries and associated flood risks, sediment regimes and morphology is raised by their socio-economic importance. Estuaries support or are affected by dense populations, transport, renewable energies, cooling water abstraction, aggregate mining, fishing, habitats, agriculture, waste disposal, and leisure activities. They face change: in freshwater runoff, sea level and sediment affecting flood risk. Outcomes depend on hydrodynamics and sediments. However, the sediment regime is challenging to predict.

Models are needed to predict changes in estuaries over many decades, for management and to assess future flood risk. This challenge for estuarine morphology studies is the subject of the Defra/EA UK Estuaries Research Programme (ERP) and the component project FD2107 *Development of estuary morphological models*. The ultimate goal is to provide estuary modelling tools and algorithms for planning and management.

Several approaches to predicting morphology have been proposed. "Bottom-Up" (B-U) process-based models are mathematical (probably numerical), spatially-resolving and predictive (probably time-stepping); they use fluid-dynamical and related equations for hydrodynamics, sediment transport and evolution of the bed. Thus B-U models represent our basic understanding of the dynamics underlying morphology. However, their ability and stability for long-term predictions is doubtful. "Top-Down" (T-D) approaches range over concepts of accommodation space; trend analysis; sediment budgeting; form characterisation; regime relationships; tidal asymmetry; equilibrium along-axis profile; translation or "rollover" with rising sea level. Such approaches may be stable for long-term predictions but some concepts (regime relationships, equilibrium) are in principle limited to their basis in data; the extent to which they can be extrapolated is uncertain; they may also lack a time-scale for evolution. "Hybrid" approaches combine T-D and B-U elements. [Typically, a T-D-concept equilibrium state constrains the form of evolution and is approached with rates and distributions provided by B-U models]. An inverse method uses a sequence of bathymetries to relate bed evolution to solution of a B-U-based diffusion-type equation.

Here we aim to test the relative merits of different models and approaches across this range, by an intercomparison and evaluation of model predictions for future morphologies. We report on applications to eight UK estuaries, permitting comparison between models in varied contexts. After describing the models (Section 2) and scenarios (estuaries and applied variations in sea level, etc., Section 3), results are presented for each model in turn relative to the simplest (Section 4). Behaviours common to models and discrepant between models are discussed in (Section 5), along with possible reasons and limits to predictability. Conclusions and scope for future work are given in Section 6.

2. The models

The different models and types are listed in table 2a (along with the estuaries to which they were applied). More details about the models themselves are tabulated in table 2b; here we give an outline for each.

Table 2a Models, estuaries and their characteristics in the intercomparisons. Entries Y *show the estuaries in which each model was run.*

Model	*Type*	*Reference*	*Thames*	*Blackwater*	*Humber*	*Mersey*	*Dee*	*Ribble*	*S'ton Water*	*Tamar*
Analytical Emulator	Hybrid	Prandle (2006)	Y	Y	Y	Y	Y	Y	Y	Y
Hybrid Regime	T-D	Wright and Townend (2006)	Y	Y	Y	Y			Y	
"2.5-D"	B-U	Lane and Prandle (2006)				Y	Y	Y		
ASMITA-type	Hybrid	Rossington and Spearman (2007)	Y							
SandTrack	Hybrid	Soulsby *et al*. (2007)	[S]Y							
TE2100	Trend	HRW (2006d)	Y							
Realignment	process	Spearman (2007)		Tollesbury Creek						
Inverse	Hybrid				Y					
Estuary properties *(From Future-Coast database)*										
Spring tidal range (m)			5.3[T]	4.6	6.0	8.9	7.6	7.9	4.0	4.7
Mean river flow (m^3/s)			66	3.8	234	67.1	31.2	33.3	18.1	27
Length (km)			100	21.2	144.7	45.6	37.0	28.4	20.2	34.1
HW Area (km^2 as represented by Analytical Emulator)			193	46.1	618	194	99	119	38.6	37.7
Intertidal Area (km^2)			52[I]	27.8	455	118	43	107	13.8	18
Marsh Area (km^2)			2.1[M]	11.0	14.2	8.5	21	22	3.6	3.6

[I]TE2100 area 42km^2 above 0m Chart Datum, plus ~10km^2 for Benfleet and Holehaven Creeks. ABPmer CHaMPs area above mean LW is 47km^2.

[M]ABPmer CHaMPs.

[S]The SandTrack model is primarily applicable (only) to the sandier parts of the Outer Thames. Hence the model results were not really comparable with the other model results focused on the estuary landward of Southend.

[T]Tidal range at the Thames mouth; 6.7 m range at Tower Bridge.

Table 2b Model characteristics.

Aspect \ Model	***Emulator***	***Hybrid Regime***	***"2.5-D"***	***ASMITA-type***	***SandTrack***	***Realignment***	***Inverse***
Type	Hybrid	Hybrid	B-U	Hybrid	Hybrid	Process	Hybrid
Source, Reference	POL & UoP Prandle (2006)	ABPmer Wright and Townend (2006)	POL Lane and Prandle (2006)	WLDelft, HRW, ABPmer Rossington and Spearman (2007)	HRW Soulsby *et al*. (2007)	HRW Spearman (2007)	UoP
Origins, Functionality *Processes*	Theory for estuary dimensions related to river flow, tidal range;	Regime theory constrains 1-D depth-integral hydrodynamic	2-D depth-integral marine dynamics, wetting & drying, friction→**u**(z);	To predict tidal basin morphology in context; "outside" and aggregated	2-D depth-integral marine dynamics, wetting & drying, sand erosion,	To predict small shallow area morphology after realignment.	To characterise morphological change by 2-D diffusion equation

	based on 1-D depth-integral hydrodynamics	results to predict new morphology	concurrent Lagrangian particle transport (w_s; random ↕ α K_z)	channels, intertidal, delta elements. Raised sea level → accommodation space; demand for sediment transport between elements	Lagrangian transport, deposition, burial; deposition changes bed	Depth-integral hydrodynamics, wetting & drying, waves, suspended sediment, w_s, diffusive transport	(sed. transport + continuity) plus "source" (analysed; represents all non-diffusive phenomena)
Dimensions	Along estuary; uniform triangle cross-section	Along estuary; cross-section statistics	x, y, z, t; C grid	Connected aggregate elements; t	x. y, t; shallow	x, y, t; shallow	x, y; t
Limits	Salinity control by mixing. No wind, waves	Not stratified No wind, waves	Not stratified Non-cohesive single sediment	Coefficients need calibration on past data	Not stratified Sandy sediment Duration versus resolution	Not stratified, no wind, single sediment, initial bed not eroded	Needs bathymetry often enough over a long period
Updating	No	Yes, unclear rate	No	Yes	Yes	Yes	No
Fixed? Evolving?	Fixed side slope, evolving depth	Evolving depth, breadth, flow	Fixed depths Evolving flow, SPM	Evolving volumes, areas of aggregate elements	Evolving flow, sand transport, depth	Evolving flow, waves, depth	Fixed diffusion, evolving depth (*c.f.* datum)
***Inputs**: depth (x &/or y)*	Mean depth, mean side slope (Future-Coast)	Cross sections, Holocene & hard surfaces	Depth (x,y) on grid	element volumes, areas from depth (x,y)	Depth (x,y) on grid	Depth (x,y)	Measured depths (*c.f.* datum), gridded
Estuary length	Future-Coast	From sections	From depths	n/a	From depths	From depths	Chosen area
Grid (resolution)	n/a	Choice O(100m)	Choice ~ 120 m	Choice of number of elements	Varied along estuary, 0.25–5 km	Choice O (100 m)	30m x 30m uniform square
Base sea level, tide range	Present MSL(see 2.1), M_2 & S_2	Present MSL, M_2, S_2	Present MSL, M_2 & S_2	Present MSL & tides	Present MSL, M_2 & S_2	Present MSL & tides	n/a
River flow	Mean (F-C /CEH)	Mean	Present mean	Mean	Not applied here	n/a	n/a
Sediment sources, type	Implicit, muddy; Emulator determines W_s.	Implicit as needed to maintain regime	Marine boundary only. Settling W_s	Marine boundary, river. Settling W_s	"seeded" + bed erosion	As needed to maintain balance	n/a
Erosion formulation	n/a	n/a	rate α bedstress	n/a (implicit to supply diffusive transport)	Soulsby (1997); rolling, hopping etc	linear in bed stress	n/a
Boundaries	Across mouth	Across mouth	Across mouth	Across mouth	Across mouth	entrance to area	Estuary boundary
Boundary conditions	MSL, M_2 & S_2	MSL, M_2 & S_2	MSL, M_2 & S_2, $\partial C_{sed}/\partial x = 0$	MSL, sediment concentration	MSL, $M_2 + S_2$, no sand influx	MSL and tides	n/a
***Output** fields*	Volumes / Areas	elevation,	elevation, currents	Volumes / Areas	elevation, currents,	Currents (x,y,t),	Grids of source

	C_{sed}	currents (x); depth (x,y,"t")	(x,y,z, t), Particle fields	of aggregated elements	depth (x,y,t), Particle fields	waves (x,y); C_{sed}, depths (x,y,t)	functions, depths (*c.f.* datum)
Scenarios *- baseline*	Present MSL Mean, spring & neap tides	Present MSL and tides	Present MSL, M_2 & S_2 tides. No wind, waves, or river	Present MSL and tides	Present MSL and tides	Present MSL, tides, waves	n/a
Change to m.s.l.	+ 0.3 m, + 1 m	5-yr increments @ +6, 20 mm/yr	+ 0.3 m, + 1 m	+ 0.3 m, + 1 m and faster rates	+ 0.3 m	n/a	n/a; continues past trend
(50-year) Extreme level	+ Flather *et al*. (2001) as MSL	n/a	As MSL, + 1.732 m	n/a	n/a	n/a	n/a
tides	+ 2%	+ 2%	+ 2%	n/a	n/a	n/a	n/a
Changed river flow	+20%	+20%	n/a	n/a	n/a	n/a	n/a
Waves	n/a	n/a	5, 9, 10, 11, 20m/s winds → bed stress	n/a	n/a	computed	n/a
Combinations	Tide range+2% & MSL + 0.3, 1m	Tide range+2% & MSL + 0.3, 1m	Tide range+2% & MSL + 0.3, 1m	n/a	n/a	n/a	n/a
Properties predicted *- areas*	Intertidal = HW-LW areas	Intertidal = HW-LW areas	Intertidal = HW-LW Marsh = HAT–HW	of aggregated elements	Evolved morphology	Can be inferred from depth(x, y, t)	Grid of depths (*c.f.* datum)
volumes	As areas	As areas	As areas	of elements	As areas	As areas	As areas
convexity $(A_{HW}+A_{LW})/2A_{MSL}-1$	n/a	Yes	Across estuary (only)	n/a	No	n/a	Could be inferred from depth (x, y, t)
SPM/tide in/out	C_{sed}	n/a	Mean per spring-neap cycle	n/a	n/a	Determined by equation for C_{sed}	n/a
Characteristic times	Flushing time T_F, Infill time T_F/C_{sed}	n/a	Potential for infill and flushing times	Time to dynamic equilibrium	Potential for flushing time	Potential for infill time	Empirical from past time-series
To use *- range*	Whole estuary; decades	Estuary or reach; decades	Estuary or coastal sea; hours - years	Whole estuary; decades	Estuary or coastal sea; days-decades	Flooded sub-area; months-decades	Estuary or reach; decades
validation	This report	This report, TE2100	Mersey: Lane and Prandle (2006)	Van Goor *et al*. (2003), TE2100, this report	This report	Tollesbury Creek: this report	Humber: this report
Documentation	This report	ABPmer R1365	Lane and Prandle (2006) / POL	HRW TR162 ABPmer R1373	HRW TR159	HRW TR157	UoP
Accessibility	Open	Open; uses proprietary flow	Open	Open as developed	Proprietary; open extension "Morpho"	Open; proprietary flow model used	Open

2.1 The *Analytical Emulator* is largely based on one-dimensional equations of axial momentum and continuity (Prandle, 2006). It assumes (as commonly observed) that tidal amplitudes are broadly uniform along estuaries. On this basis, changes of phase, along-estuary wave-number and current U are functions of the tidal range Z and estuary depth D (and of friction coefficient and tidal frequency, but these may be considered as uniform between the estuaries considered; Prandle, 2004). Along-estuary change of depth $\partial D/\partial x$ is a function of the same variables. Thus Prandle (2004) derived estuary length as a function of the tidal range Z and estuary depth D (by integrating $\partial D/\partial x$ to where D=0). Neglecting axial mixing, he also related saline intrusion length to the remaining variables – depth, bed roughness, current U and river flow Q_f – eventually deriving (Prandle, 2004)

$$D_{\text{Estuary mouth}} = 12.8\,(Q_f\ a)^{0.4}$$

where *a* is the side-slope of the estuary (triangular cross-section assumed). Thus the Emulator partly explains how estuarine bathymetries have developed in response to tidal and riverine inputs (Prandle *et al*., 2006). A modification by Manning (2007a) allows time-averaged river flow $\langle Q_f \rangle$ input values to estimate the average estuary depths $\langle D_{AE} \rangle$:

$$\langle D_{AE} \rangle = 12.8\,(\langle Q_f \rangle * a_{\text{mean}})^{0.4} * M.$$

Baseline conditions were from the newly enhanced Future-Coast database of UK estuaries (Manning, 2007b). This was used to compute the actual mean estuary depth and width. From these were estimated the estuary side slope. The Emulator assumes that the actual estuary length (from the enhanced FutureCoast database) and side slope (so calculated) remain constant. The assumed constant single side slope (everywhere in the estuary) involves a compromise between correct HW, LW or intertidal volumes or areas; in general not all of these can be correct. A mean estuary depth $\langle D_{data} \rangle$ was computed for a specific estuary; the Emulator-derived $\langle D_{AE} \rangle$ was equated to $\langle D_{data} \rangle$ by choice of the calibration coefficient *M*, so providing a good starting position. $\langle D_{AE} \rangle$ is equivalent to a mean sea level (MSL) datum. This allowed the Emulator equations for the breadth, $\langle D_{AE} \rangle$ and associated channel bathymetry, to be solved reasonably accurately. In this formulation the morphology responds (in depth $\langle D_{AE} \rangle$ and width proportional to $\langle D_{AE} \rangle / a_{\text{mean}}$) only to changes of river flow $\langle Q_f \rangle$ among the scenario changes.

Sea level rise was imposed on the Emulator channel geometry giving new values for estuary volume and area. All of the change in water level to 2050 (0.3m or 1m) was imposed at once, rather than in real time in parallel with resulting changes in bathymetry.

For infilling by suspended particulate matter (SPM), a half-life in suspension is a function of settling velocity W_S, estuary depth D and diffusivity proportional to UD, i.e. a function of W_S, D, Z (current U is a function of D, Z). Hence the SPM concentration C is a function of W_S, D, Z. A minimum infilling time was estimated from flushing time and mean concentration $\langle C \rangle$ (Prandle, 2004); $\langle C \rangle$ increases with tidal range but is assumed constant for the scenarios with raised sea level. Manning (2007a) gives more detail.

2.2 The *Hybrid Regime* model (ABP; Wright & Townend, 2006) allows application of an empirical "regime theory" relationship with a 1-D hydrodynamic model (ISIS or Mike11), in order to predict long-term (decades to centuries) change within estuaries. It also takes account of (underlying) hard surfaces; cross-sections describing the underlying Holocene surface were generated; where this is unknown, a fixed depth was assumed based on existing data sets.

The 1-D hydrodynamic model outputs water level, velocity and discharge and is calibrated against measured or predicted water levels and velocities. The empirical regime relationship is generated from the baseline flow results of the 1-D model, assuming that:

- the estuary will achieve some form of equilibrium state
- the existing estuary form can be characterised by an equilibrium relation (function).

Regime theory was first described for estuaries by Langbein (1963) who found relationships for cross-sectional area A, top width B and mean hydraulic depth H in terms of discharge Q:

$$A \propto Q_{max}^{\ p}, \qquad B \propto Q_{max}^{\ q}, \qquad H \propto Q_{max}^{\ r}$$

The constants (p, q, r) are obtained from fitting to the results of the initial model run. These relationships characterise the estuary morphology (e.g. cross section area along the estuary) in terms of estuary hydrodynamics (maximum discharge). In deriving this best-fit regime relationship between the peak discharge and simultaneous cross-sectional area data points, there will be scatter. Forcing the regime relationship on the existing form-discharge variation along the estuary could imply a substantial change in some of the cross-sections, before any perturbation is introduced. To avoid such changes, cross-section deviations from the best-fit regime relationship can be retained by making relative, rather than absolute, adjustments.

Then some condition in the hydrodynamic model is altered, e.g. changed water levels at the driving boundary, or addition of engineering works. The new morphological geometry is obtained by reapplying the regime relationships after the perturbation. Thus the Shell (i) reads and assesses the equilibrium state of the estuary, (ii) calls the hydrodynamic model and runs the altered simulation, (iii) calculates the change from the equilibrium condition, (iv) updates the 1-D cross-section bathymetry according to the regime conditions and constraints of the Holocene surface, using linear stretching (vertically and horizontally), (v = ii) re-runs the simulation until the regime condition is met (figure 2.2). In the runs reported here, sea-level rise was applied in 5-year increments; for each increment the model was iterated until the estuary bathymetry was within 5 per cent of the "equilibrium" bathymetry defined by regime theory; the water level was then raised by a further 5-year increment and the process repeated. (This methodology does not model the evolution of the estuary in real time in parallel with sea level rise).

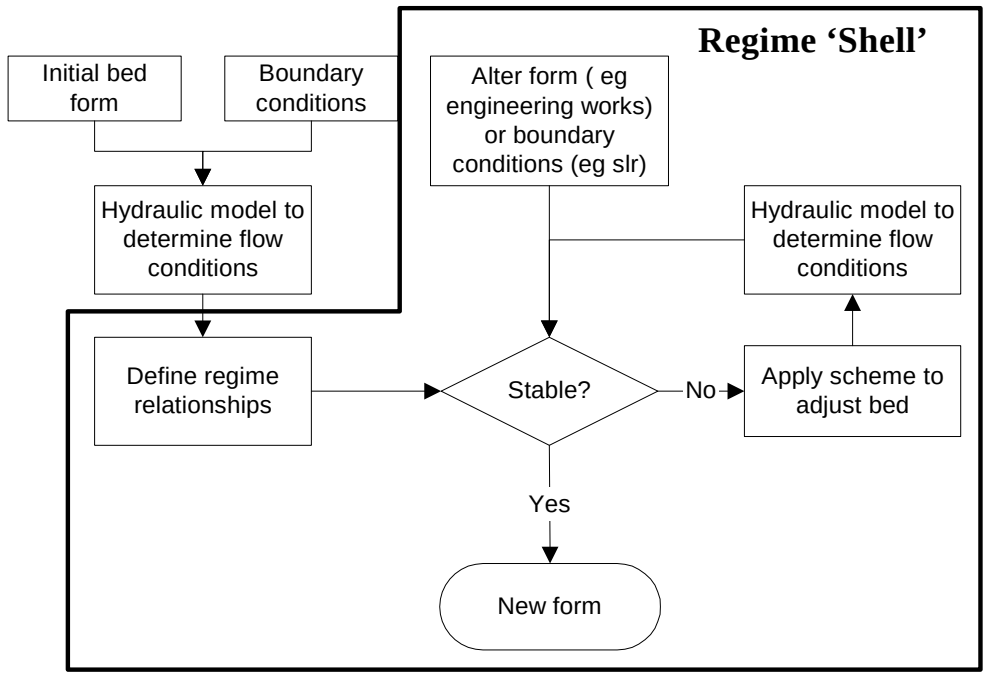

Figure 2.2 Hybrid Regime model "Shell" interactions: with 1-D hydrodynamic model and with rules applied to derive the final model bathymetry.

Cross-sections are adjusted at stage (iv) to meet the new area required to satisfy the regime relationship. The adjustment is only below the maximum water level. In addition, fixed surfaces can be defined, to represent the influence of solid geology and of structures such as sea walls, bridge piers; the adjustment routine limits where on a cross-section the erosion is allowed to take place. Application of physical constraints is critical. Without them, cross-section top widths increase under sea level rise; intertidal area increases. In reality, physical constraints prevent some sections from widening; such sections can only deepen to maintain the regime cross sectional area, provided that this is not prevented by a physical constraint. Consequently, intertidal area is lost. A section that increases in area and has no physical constraint may gain or lose intertidal area, depending on the section convexity. The adjustment takes no account of any condition in flow across the section. For the Thames, no morphological change is predicted if a minimum threshold is used at the level of "noise" or error inherent in the methodology; changes in the Thames over the 20^{th} century were within this level. Hence the Hybrid Regime model was (re-)run for the Thames Estuary without a minimum threshold for change.

2.3 The *"2.5-D"* B-U model (POL; Lane and Prandle, 2006) integrates the 2-D shallow-water equations for conservation of mass and momentum, stepping forward in time, on a finite-difference C-grid, resolution O(120 m) (for the Mersey, Dee and Ribble). Vertical structure (10 layers through the depth everywhere) is then derived from the 2-D model pressure gradient, with an assumed bed friction coefficient and viscosity (i.e. the vertical structure is controlled by the 2-D solution; vertical diffusivity = vertical eddy viscosity = fUD, where f is the bed friction coefficient, U the tidal current amplitude and D water depth). Sediment is modelled concurrently by Lagrangian tracking of (typically) 10^5 independent particles moving with the flow; a 'random-walk' module simulates erosion, suspension and deposition. In the simulations, erosion is the conventional function of excess bed shear stress. Suspended sediment is supplied at the estuary mouth according to the flow there; particle motion is represented by random vertical excursions, magnitude $\sqrt{(2\,E\,\mathrm{d}t)}$ each time step dt, and advection horizontally with the flow. Deposition is via settling velocity; W_s dt in each time-step. Bathymetry, gridded from Lidar/echo sounder surveys, is fixed through the model run.

2.4 ASMITA (Aggregated Scale Morphological Interaction between a Tidal inlet and the Adjacent coast) was first presented as a behaviour-based model "describing morphological interaction between a tidal lagoon or basin and its adjacent coastal environment" (Stive *et al*., 1998). The model schematises a tidal inlet system, the main morphological elements being viewed at an aggregated scale (**Error! Reference source not found.**2.4). Under constant hydrodynamic forcing (in particular constant mean sea level), each element is assumed to tend towards a morphological equilibrium definable as a function of hydrodynamic forcing and basin properties (van Goor *et al*., 2003). Empirical relationships are used to define the equilibrium volume of each element (Stive *et al*, 1998).

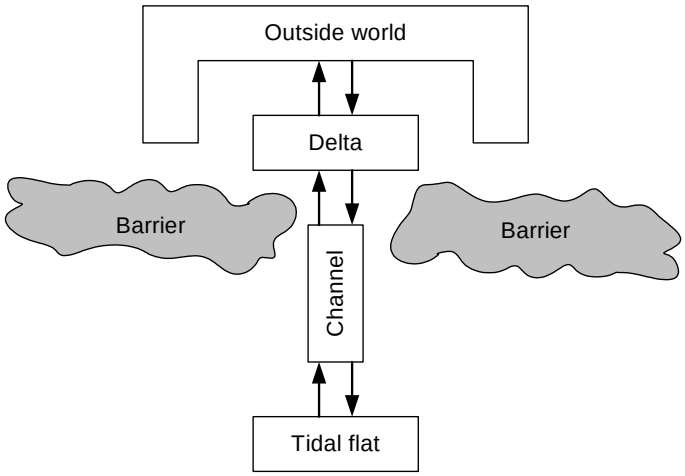

Element definitions:

Ebb-tidal Delta: Excess sediment volume above a hypothetical non-inlet shoreface

Channel: Water volume below mean low water

Tidal flat: Sediment volume above mean low water

Figure 2.4 ASMITA schematisation and element definitions (from van Goor *et al*., 2003)

Sea-level rise creates accommodation space within the estuary; the estuary becomes a sink for available sediment. ASMITA represents this by an increase in the difference between elements' actual volume and equilibrium volume, causing sediment demand. A gradient of sediment demand drives sediment transport; sediment diffuses into the estuary, changing the morphology. Hydrodynamics are represented by integral properties (tidal range, tidal prism). The morphological elements in ASMITA (intertidal area, channels, ebb-tidal delta) interact through sediment exchange. This interaction plays an important role in the morphological evolution of the whole system, as well as that of the individual elements (van Goor *et al*., 2003). If morphological elements are not present (e.g., ebb tidal delta), reduced element models can be applied. Long-term, residual sediment exchange is assumed to occur between adjacent model elements; development of the tidal inlet is assumed not to affect availability of sediment in the outside world, represented by a global equilibrium concentration (van Goor *et al*., 2003). Volume changes within elements are described by equations 2.4(1-3). Sediment is transferred between elements to satisfy mass balance equations 2.4(4-6).

$$dV_f / dt = Ws_f * A_f * (c_f - c_{fe}) - A_f * (d\xi / dt) \qquad 2.4(1)$$

$$dV_c / dt = Ws_c * A_c * (c_c - c_{ce}) + A_c * (d\xi / dt) \qquad 2.4(2)$$

$$dV_d / dt = Ws_d * A_d * (c_d - c_{de}) - A_d * (d\xi / dt) \qquad 2.4(3)$$

Here A_n is the area of element n; Ws_n is the vertical exchange coefficient for element n; c_n is the actual concentration; ξ is sea-level; c_{ne} is an element's local equilibrium concentration, defined in equations 2.4(7-9). Subscripts, *f*, *c* and *d*, refer to the tidal flat, channel and ebb-tidal delta elements, respectively.

$$\delta_{fc} * (c_f - c_c) = Ws_f * A_f * (c_{fe} - c_f) \qquad 2.4(4)$$

$$\delta_{fc} * (c_c - c_f) + \delta_{cd} * (c_c - c_d) = Ws_c * A_c * (c_{ce} - c_c) \qquad 2.4(5)$$

$$\delta_{do} * (c_d - C_E) + \delta_{cd} * (c_d - c_c) = Ws_d * A_d * (c_{de} - c_d) \qquad 2.4(6)$$

Here δ_{fc}, δ_{cd} and δ_{do} are coefficients for horizontal exchange between the flat and channel, the channel and delta, and the delta and outside world.

$$c_{fe} = C_E * (V_f / V_{fe})^r \qquad 2.4(7)$$

$$c_{ce} = C_E * (V_{ce} / V_c)^r \qquad 2.4(8)$$

$$c_{de} = C_E * (V_d / V_{de})^r \qquad 2.4(9)$$

Here V_n is elements n's current volume; V_{ne} is elements n's equilibrium volume; C_E is the global equilibrium concentration; $r > 1$ and usually r is taken as 2 in compliance with sediment transport as a third power of flow velocity (van Goor *et al*., 2003).

There is flexibility to specify many aspects of the estuary context: tidal range, equilibrium sediment concentration, water density, sediment density, sea level rise, elements (type, initial volume and area, bed slope, length, import density, bulk bed density etc.), flow/diffusion rates (connectivity) between elements. Constraints on system response (e.g. sea walls) can be represented, and known changes to element volume can be specified with their timing.

In its basic form ASMITA predicts changes in the volume of channel elements (below mean water level) and volume of intertidal flat elements (above some reference level such as mean LW springs). It does not directly predict changes of intertidal area. In application here to the Thames, changes of intertidal area are calculated by assuming that changes of surface area vary linearly with changes of intertidal volume.

To apply ASMITA to the Thames Estuary a six-element scheme was used; flats and a channel in each of three reaches (Rossington and Spearman, 2007). Equilibrium relationships 2.4(10, 11) for the channel equilibrium volume (V_{ce}) and the flat equilibrium volume (V_{fe}) were estimated from historic volume and area data. Equilibrium coefficients were selected to give the best representation of the estuary geomorphology during the period of data availability.

$$V_{ce} = a_c * P \qquad 2.4(10)$$

$$V_{fe} = H * a_f * (A_{Basin}) \qquad 2.4(11)$$

Here H is the mean spring tidal range, A_{Basin} is the basin area, a is an empirically derived coefficient; subscripts f and c refer to flats and channels respectively; P is the tidal prism:

$$P = (1 - a_f) * (A_{Basin}) * H \qquad 2.4(12)$$

$$a_f = (A_f / A_{Basin}) * (h_f / H) \qquad 2.4(13)$$

where A_f is the flat area and h_f is the equilibrium flat height.

Sediment transport coefficients Ws_n, δ_{nm}, C_E were estimated based on Wang (2005):

- Vertical exchange coefficient Ws_n: same order of magnitude as, and proportional to, the average fall velocity (in m/s);
- Coefficient r: equal to the power law in the sediment transport formula; typically 3 for mud and 5 for sand;
- Horizontal exchange coefficient δ_{nm}: estimated based on the area available for sediment exchange A, the length scale of exchange L and the diffusion coefficient D: $\delta = DA/L$; the diffusion coefficient D is given by $D = u^2H/Ws$ where u is the peak velocity and H is the average water depth.

Once the other parameters have been estimated, the Global equilibrium concentration C_E is used to fit the model to the observed morphological time scale. Van Goor *et al* (2003) suggest that the uncertainty associated with these parameters is approximately +/- 50 per cent. The ASMITA model was calibrated to the historical variation in Thames Estuary morphology using the historical variation in dredging, disposal, sewage inputs and fluvial input collated by the *Thames Estuary 2100* studies (HRW, 2006a; Rossington and Spearman, 2007).

2.5 The *SandTrack* model (HRW) was developed before the start of FD2107, for Lagrangian particle-tracking of sand-grains including bedload, suspended load, incipient motion, burial and re-emergence processes. The model operates by tracking the movement of "tagged" grains of sand, each representative of many billions of similar grains. Runs for typically a few weeks to a few decades predict where the tagged grains go to. SandTrack has been

extended in FD2107 to associate a volume of sediment with each tagged grain, and deposit it on the bed in a diffuse fashion as a sediment "lens" with a defined maximum thickness and extent. The sum of the lenses gives the morphodynamic development of the estuary. By repeating this process at intervals, with hydrodynamics re-calculated for each interval, this has become a Hybrid morphodynamic model: *Morpho-SandTrack.*

The characteristic dimensions of sediment lenses have been calibrated against the well-established Van Rijn sediment transport formula, by running Morpho-SandTrack for an idealised flume case with various steady current speeds and sediment grain-sizes. The present model does not include the effects of waves, although it would not be difficult to add them; they are already included in the original SandTrack. Wave effects can re-distribute sediments, especially in the outer parts of an estuary. In contrast to the "2.5-D" model with particle tracking, Morpho-SandTrack applies to coarser sediments (sands, not silts or muds), uses fewer particles ($> 10^4$ rather than $> 10^5$), runs for much longer (decades rather than days) and updates the flow field in response to the changing bathymetry. An advantage over other Hybrid models is that the *source* of deposited sediment (on tidal flats, saltmarshes) is known as well as its thickness. The tagged particles can carry a marker to indicate pollution with heavy metals, for example (not implemented in FD2107).

The newly developed and calibrated Morpho-SandTrack model was tested in the Thames Estuary, to predict morphological changes over 50 years, with one-year update intervals for the bed and the flow. Being concerned with the movement of sand, SandTrack covers primarily the outer estuary (where the sand is). It requires repeated runs of a 2-D model of the Thames and outer estuary; TELEMAC was used. Resolution varied along estuary, ~0.25 km in the narrower reaches to ~5 km at the offshore boundary. It is attractive to coarsen the flow model mesh to reduce run times (for the hydrodynamics and so for the morphological simulation overall). This has to be balanced against the need for sufficient resolution to compare with observed trends.

2.6 *TE2100 Historical Trend Analysis* (HTA; HRW) derived 2030 bathymetry for the Thames by calculating the change between the 1970 and 2000 bathymetries and adding the change in bed level between 1970 and 2000 to the 2000 bathymetry. However, this alone is not realistic:

- Changes in channel position often lead to large vertical changes: a few metres. Further such "accretion" gives unrealistic banking on the lower intertidal; further such "erosion" gives unnatural channel deeps near the foreshore.
- Subtidal changes due to dredging or other capital works should not be extrapolated.
- The bathymetry of declared navigation channels is managed, not natural.

Hence the extrapolated bathymetry was further modified as follows:

- No subtidal erosion of more than 2m was allowed;
- Subtidal accretion was not allowed above 0mOD (roughly mid-tide).

Moreover, two geometries were prepared to span possible navigation management strategies:

- Geometry 1: subtidal changes seaward of Charlton were defined as above;
- Geometry 2: as Geometry 1 except that no change in bathymetry below -5mOD was allowed seaward of Charlton (depths in the navigable river maintained as *status quo*).

2.7 The *Realignment* model (HRW) was developed, partly in FD2107, to predict local changes in morphodynamics and evolving habitats resulting from managed realignment. Sites have specific complexities, with significant roles of tides, waves, sediment, vegetation and biology at small spatial and temporal scales. The model builds on the successful

conceptual approach to habitat development of di Silvio (1989), di Silvio and Gambolati (1990) for lagoons. It is Hybrid, combining bottom-up and top-down aspects to describe the essential inlet functioning; it can incorporate effects of waves and vegetation, and allows future increases in complexity as knowledge of these and other processes develops.

A shell script controls (Figure 2.7.1): application of a flow model; a wave model; a program which derives equilibrium concentrations and time-averaged dispersion characteristics; a "di Silvio-type" time-averaged sediment transport model originally developed by Galappatti and Vreugdenhil (1985):

$$E = w\,(C_E - C) \qquad (2.7.1).$$

Here E is the net erosion (a negative value indicates deposition), w is the settling velocity, C_E is an equilibrium concentration and C is the actual concentration. The model sequence is:

a) Set up initial bathymetry
b) Work out time-averaged wave heights and periods at every point in model domain
c) Use TELEMAC-2D flow model to get flow conditions in set back field
d) Post-process the flow and wave results; (i) for a spatial distribution of time-averaged diffusion coefficients (Dronkers *et al,* 1982); (ii) for a spatial distribution of time-averaged equilibrium concentrations C_E incorporating wave effects (using the wave model of Young and Verhagen, 1996); (iii) save derived values in a form which can be used as input to SUBIEF-2D
e) Run SUBIEF-2D, a time-averaged sediment transport model; (i) use derived time-averaged diffusion coefficients and zero residual currents [i.e. diffusive process only]; (ii) use (2.7.2) for sediment transport; (iii) update bathymetry during simulation
f) Extrapolate predicted change in bathymetry from SUBIEF-2D model over a much longer time step and save results
g) Bathymetry is used as basis for another run of the TELEMAC-2D model – go to "b".

Here TELEMAC-2D is a finite element model which solves the shallow water equations. SUBIEF-2D is a suspended sediment model, the mud transport module of the TELEMAC suite. For this study, the code was altered: (i) the dispersion coefficients and equilibrium concentrations calculated from the flow model results were read by the SUBIEF-2D model; (ii) the calculations of erosion and deposition were changed from the formulations of Krone (1962) and Partheniades (1965) to that of Galappatti and Vreugdenhil (1985).

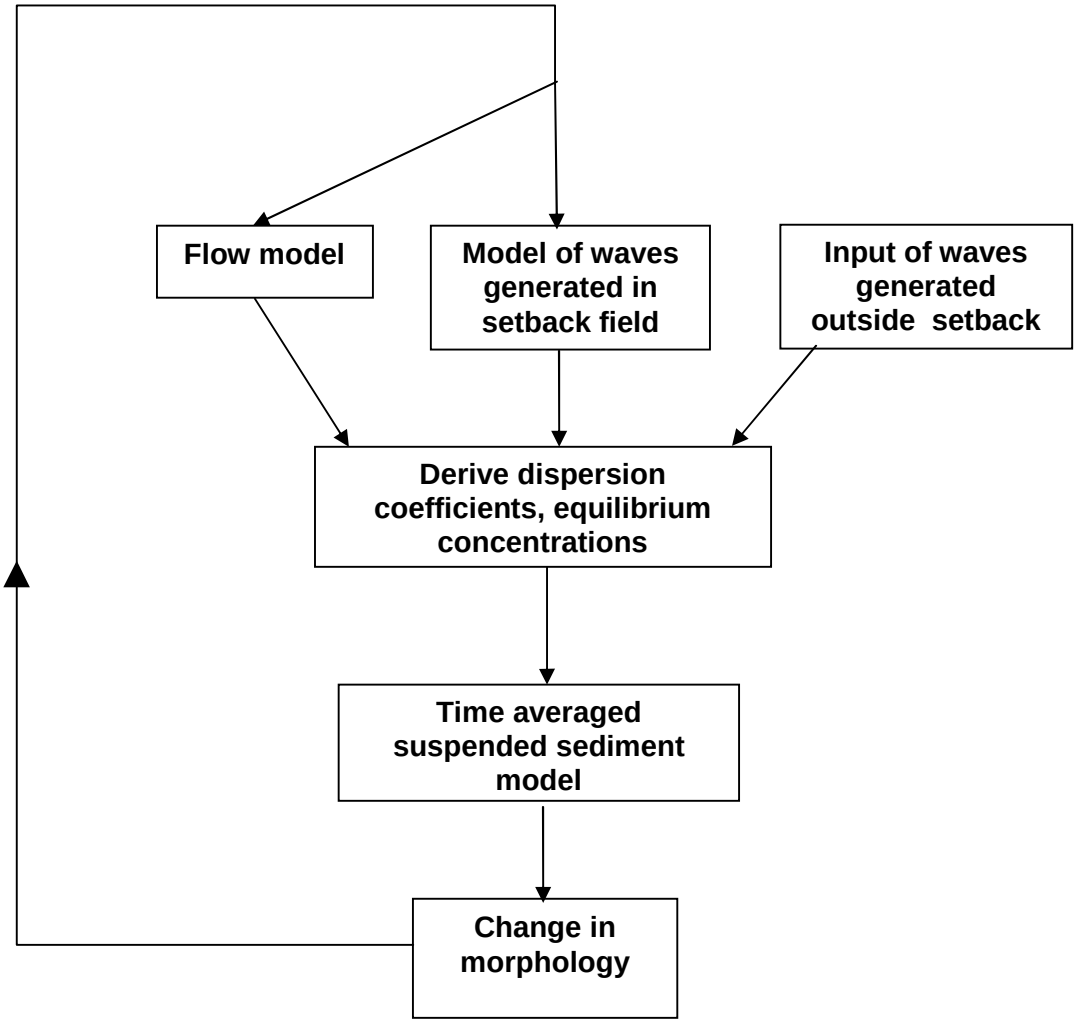

Figure 2.7.1 Basic structure of Realignment morphological model

As there is no residual transport in setback fields the model, the time-averaged transport into the field is modelled as a diffusive process and controlled by the (spatially varying) diffusion coefficient. The diffusion coefficient is assumed to be proportional to the square of the time-averaged current speed within the setback field (Dronkers *et al*, 1982). The time-averaged sediment transport model then uses the distribution of diffusion to model the movement of sediment into the setback field. The absolute magnitude of the diffusion coefficients is calibrated along with the other model parameters.

An equilibrium concentration has no empirical basis on a "virgin" managed realignment site. It is derived (as a time-average) by equating the deposition occurring during slack water with the erosion occurring during the rest of the tide:

$$\int_{\tau>\tau_e} M_e(\tau-\tau_e)\,dt = \int_{\tau<\tau_d} w_s C\left(1-\frac{\tau}{\tau_d}\right)dt = C_E \int_{\tau<\tau_d} w_s\left(1-\frac{\tau}{\tau_d}\right)dt \qquad (2.7.2)$$

The value of C_E at any location thus depends on the variation of current speed and wave action and the friction parameter (which give the value of bed shear stress), the thresholds of erosion and deposition, the settling velocity and the erosion rate. There is uncertainty in all of these. To some extent, values can be estimated from typical values in the literature, but there will always be appreciable uncertainty in the value of C_E.

Processes not currently included in the model as run here include:

- The effect of biology on bed shear stress;
- Erosion of the initial bathymetry (re-erosion of deposited sediment *is* reproduced);
- Erosion (via geotechnical processes) of the sea walls at the entrance to the set back site;

The Realignment model was applied to the case study of Tollesbury Creek in the Blackwater Estuary. Modelling of evolution of a managed realignment here, compared with the observed evolution, is described in detail in Spearman (2007). Sensitivity studies showed significant dependence on internally-generated waves and bed roughness, and especially the benefit of fine model resolution.

2.8 The *Inverse model* (UoP) uses a 2-D diffusion-type morphological equation (for the height of the bed level as a function of position and time) with "source":

$$\partial h/\partial t = K(\partial^2 h/\partial x^2 + \partial^2 h/\partial y^2) + \text{source} \qquad (2.8).$$

[Such an equation is suggested by combining sediment transport having a down-slope bias with a sediment continuity equation]. The "source" represents the aggregate of all non-diffusive phenomena that lead to long term evolution of estuary morphology. In practice the diffusion coefficient is supposed spatially uniform and constant in time; any effects of variable diffusion coefficient are included in the source function.

The model depends on measured bathymetries covering a long period, frequent enough not to alias changes in form, works (training walls, etc.) or management (e.g. dredging). Bathymetry at two times allows "inversion" for the time-averaged source during the interim.

The Inverse model was applied to the Humber. Sensitivity of the source function to the diffusion coefficient was investigated by reconstructing the source function with ± 50 per cent of the chosen value. There was no apparent difference to the structure of the source function when the diffusion coefficient was varied.

For bathymetry data at sufficiently frequent intervals, Empirical Orthogonal Function (EOF) or Principal Component analysis of the source identifies trends in bathymetric change; it should show any spatial and in particular temporal structure to be exploited for prediction. This technique is widely known; further details can be found in Horrilo-Caraballo and Reeve (2002), Reeve and Horrilo-Caraballo (2003). Here, the first Component contains almost 92 per cent of the source function, and indicates its near-constant strength through time.

To predict future morphological evolution, the diffusion-form bed evolution equation (2.8) was used. The diffusion coefficient was assumed constant and the source function was taken as the time-average first Component, in effect extrapolating past historical behaviour.

As well as the Humber, it had been intended to apply the approach to the Thames and Mersey. However, UoP concluded that results for the Thames and Mersey would not be particularly meaningful; bathymetry was not at intervals short enough for the computed forcing term to change fairly smoothly from interval to interval.

3. The scenarios

Altogether the models were run for eight estuaries as shown in table 2a: Thames, Blackwater, Humber, Mersey, Dee, Ribble, Southampton Water, Tamar. Intercomparisons of model predictions were generally for 2050. For the Thames Estuary, comparison has been made for

2030, to take account of work previously undertaken for the TE2100 study. In terms of area (table 2a), the Humber is by far the largest estuary; there is a middle group comprising the Thames, Mersey, Dee and Ribble; the Blackwater, Southampton Water and Tamar are "smaller" estuaries (but still tens of km^2 and so sizeable by UK standards; the Ribble would also be "smaller" if judged by area at low water). All have large tidal range by world standards; the range is greatest for the Mersey, Dee and Ribble. Interestingly, most have a similar ratio of river flow to area, but Blackwater river flow is relatively small and the Tamar's is relatively large (this is the only ria; the estuary area is constrained). The Thames and Tamar are relatively long for their area (and therefore narrow). A large proportion of the Ribble area is intertidal; the proportion is least for Southampton Water and the Thames. The proportion of saltmarsh is large for the Dee, Blackwater and Ribble, and least in the Thames.

3.1 The *Thames* Estuary is long (100 km). Tidal range increases up the estuary. There are large intertidal areas in its lower reaches and a heavily modified channel in its upper reaches. Along most of the Thames Estuary, MHWS intercepts tidal defences. Hence under climate change, MHWS area would hardly increase (less than 1 per cent). The Thames Estuary 2100 (TE2100) study includes morphological prediction techniques and their application to the Thames Estuary. From these and a detailed atlas of morphological change over the last century, two 2030 morphologies were developed by extrapolating recent historical changes. Being based on data, this method of prediction represents a baseline for predicted 2030 morphology; trends arising from this prediction ought to be reflected in the other models. In the absence of morphological response, the predicted future intertidal area should provide an upper limit on losses under the different climate change scenarios; inclusion of morphological response would act to decrease the losses. Table 3.1 shows TE2100-estimated changes if there were sea level rise only (no morphological change), if there were change in morphology only (no sea level rise) and for change in morphology and sea level rise combined. These illustrate the possible range of outcomes: +/- 1 km^2 change in intertidal area.

Table 3.1 Volume and surface area of historical and future bathymetries in the Thames Estuary (HRW, 2006b,c)

Bathymetry	*Surface area (km^2)*		*Intertidal Area (km^2)*	*Volume (km^3)*		*Tidal volume (km^3)*
	LW	*HW*		*LW*	*HW*	
1920	82.4	125.8	43.4	0.5639	1.2608	0.6969
1970	77.2	117.5	40.3	0.5212	1.1779	0.6567
2000	73.8	117.7	43.9	0.5203	1.1575	0.6372
2030 (just effect of sea-level rise)	74.7	117.7	43.0	0.5302	1.1725	0.6423
2030 Geometry 1* (just effect of morphology)	72.6	117.6	45.0	0.5398	1.1462	0.6064
2030 Geometry 2* (just effect of morphology)	72.5	117.6	45.1	0.5245	1.1339	0.6094
2030 Geometry 1* (sea-level rise + morphology)	72.9	117.6	44.7	0.5518	1.1675	0.6157
2030 Geometry 2* (sea-level rise + morphology)	72.9	117.6	44.7	0.5364	1.1552	0.6188

* Geometry 1 extrapolates the subtidal bathymetry assuming there is no overall effect of dredging on the morphological trend.
Geometry 2 assumes that because of dredging the channel-bed part of the subtidal area will remain constant in depth over time.

3.2 The *Blackwater* Estuary is relatively small (21 km long). River inflow (Blackwater and Chelmer) is particularly low, but marsh occupies a large proportion of the total estuary area. Whilst this estuary has not been the focus for major studies in recent times, managed realignment projects have been undertaken, notably the Tollesbury managed realignment about which there is considerable information. The realignment site is at the end of a 1 km creek, part of Tollesbury Fleet in the Blackwater. Mean-spring tidal range in the creek is about 4 m; most of the creek dries out at low water. The Realignment model was applied to the realignment site; the Analytical Emulator and Hybrid Regime model were applied to the whole estuary.

3.3 The *Humber* Estuary in north-east England is the largest of the eight estuaries studied here, with length 81 km (plus additional channel length in the Don and Trent, to a total 145 km). Freshwater runoff to the estuary is via the Ouse, Don and Trent (mean flows exceeding 120, 16, 95 m^3/s respectively). The tide amplifies as it propagates up the estuary. The Humber has areas of saltmarsh, and a complex (almost braided) channel system in its lower reaches. There has been a wealth of research on the estuary; more information is the Humber Estuary Shoreline Management Plan (EA, 2000) and the Humber Estuary Geomorphological Studies Reports (Murray and Pethick, 1999).

3.4 The *Mersey*, *Dee* and *Ribble* have the largest tidal ranges of the estuaries considered; the Ribble has the largest proportion of intertidal area; the Dee and Ribble have relatively large areas of saltmarsh. Bathymetry for the Mersey, Dee and Ribble was gridded from Environment Agency Lidar/echo sounder surveys in 2002, 2003, 2004 respectively. "2.5-D" model boundaries were generally located in water depths of about 20 m: Mersey – E-W line at mouth between New Brighton and Gladstone Lock; Dee – north from Hoylake and north from Rhyl with northern boundary through Hilbre Swash; Ribble – west from Lytham and west from Formby Point to N-S line approximately 3 km offshore. Tidal amplitudes (M_2, S_2 in m) were taken as: Mersey – 3.04, 0.98; Dee – 2.92, 0.95; Ribble – 2.95, 0.88. A 50-year extreme surge for Liverpool, +1.732 m (Flather *et al*., 2001), is derived from observations and a 40-year storm surge model run. River flows used were: Mersey and Dee 150 $m^3\ s^{-1}$, Ribble 100 $m^3\ s^{-1}$. Fine sediment (settling velocity w_s = 0.0005 m s^{-1}) was assumed in the "2.5-D" model. Wind speed (if applied, with the effect of wave-enhanced bed stress) was 10 m s^{-1} from the west, other scenarios being 5, 9, 11 and 20 m s^{-1}.

3.5 *Southampton Water* is 19 km long with Itchen and Hamble sub-estuaries (length 7, 8.6 km respectively). Mean river inputs to the three (sub-)estuaries are 12.3, 5.6, 0.4 m^3/s respectively. Mean width of Southampton Water is about 2 km sea-ward of the Itchen. Tidal range at the mouth, 3.75 m, is moderate by UK standards. A "double high water" results as arrivals via the two sides of the Isle of Wight are made distinct by non-linear steepening.

3.6 The *Tamar* Estuary is small in area but relatively long and with large river inflow; of the eight, it is the only ria. It was modelled only by the Analytical Emulator.

3.7 Various scenarios are intended to represent possible effects of climate change 50 years hence [as used in TE2100, CDV2075; referring to UKCIP02, IPCC(2001), Defra (2003); the scenarios were defined prior to issue of the latest government guidelines (Defra, 2006)]:
Mean sea level: baseline as at present; rises of 0.3 m (realistic over 50 years), 1 m (extreme)
50-year extreme level: in practice applied as a constant addition to sea level
Tidal range: baseline as at present; an increase of 2 per cent (Flather *et al*., 2001)
River flow: baseline as at present; an increase of 20 per cent

Waves: (a) as enhanced bed stress associated with wind (nominal value and ± 10 per cent)
(b) as forced by eight wind scenarios representing the distribution of conditions in Liverpool Bay (for the Mersey, Dee and Ribble; see Annex A1 *SWAN modelling of Liverpool Bay including Mersey, Dee and Ribble*).

4. Results

In this section we take the models in turn to discuss results in relation to those of the Analytical Emulator. This choice of comparator is not to prejudge its merits, but (i) the Emulator is simplest for interpreting results; (ii) it was run for all eight estuaries and therefore always has results available for comparison. For the Thames, table 3.1 provides an additional comparator.

4.1 Analytical Emulator

Many results are summarised in table 4.1: changes in low water (LW) and intertidal volumes, for rises in mean sea level (MSL); changes in flushing times; changes of infill times. Other results for some estuaries in subsequent tables (comparisons) include high water (HW) volumes, LW and HW areas and suspended sediment fluxes.

Table 4.1 Emulator characteristics and results for the estuaries.

Estuary / ***Scenario / Characteristic***	*Thames*	*Black-water*	*Humber*	*Mersey*	*Dee*	*Ribble*	*S'ton Water*	*Tamar*
Baseline length, km	82.5	21.2	144.7	45.6 km	37.0	28.4	20.2	34.1
$<D_{AE}>$, m	6.4	6.8	5.5	7.5	23.1	4.3	11.5	8.8
Mean width, km	1.6	1.6	2.9	2.8	2.3	2.3	1.6	0.90
LW volume, km^3	0.124	0.051	0.3	0.106	0.73	0.0049	0.130	0.079
HW volume, km^3	0.898	0.209	2.5	1.11	1.31	0.464	0.261	0.204
LW area, km^2	72	22.7	223	60	74	12	27.2	23.5
HW area, km^2	193	46.1	618	194	99	119	38.6	37.7
Hence intertidal area, km^2	121	23.4	395	134	25	107	11.4	14.2
MSL + 0.3m, + 1m								
LW volume change	18.1%, 66.4%	15%, 49%	21.5%, 80%	17.7%, 64.6%	3%, 10.3%	90%, 409%	6.4%, 22%	9.1%, 31.8%
Tidal prism change	6.5%, 22.7%	4.4%, 14.6%	5.4%, 17.1%	4.0%, 13.4%	2.3%, 7.7%	7.0%, 23.3%	2.6%, 8.7%	3.4%, 11.4%
Baseline flushing[F] time, days	7	9	6.3	7.5	21.3	4.7	14.9	11.5
[E]Extreme flushing[F] time, days	11	14.5	10.2	11	25.5	8.3	19.2	14.1
Baseline mean SPM, mg/l	127	69	112	164	214	125	77	74
Baseline infill time, years	218	516	223	182	395	149	765	619
[E]Extreme infill time, years (+%)	344 (+58%)	822 (+59%)	354 (+60%)	263 (+44.6%)	467 (+18%)	259 (+74%)	976 (+27.6%)	751 (+30%)

[E]Extreme scenario for flushing time and infill time means MSL + 1m, + 50-year surge, + extra 2 per cent tide range + extra 20 per cent river flow.

[F]Different definitions of flushing and related time-scales are possible. The Emulator estimate is the time to replace by freshwater, half of the salinity content over the saline intrusion length. For the eight estuaries considered, this estimate is longer than estimates based on flushing by the tidal prism O(1 day) and less than estimates (months) based on river inflow and the whole estuary volume.

Comparison (with the Hybrid Regime model results, table 4.2) illustrates the Emulator's geometrical limitation: uniform side-slope prevents a good representation of the low water channel. Emulator LW volumes for the Blackwater are about half of the actual LW volumes; in the Mersey, the Emulator has more HW volume but less LW volume; there are also severe discrepancies in the Dee (table 4.3).

For raised MSL, the Emulator predicts equal increases in LW and HW area, e.g. by 6.2 km^2 for the Thames under a MSL + 0.3m scenario. In reality, present HW generally intercepts walls in the Thames Estuary; rises in sea level will not increase HW area (i.e. the Emulator is not realistic), but would raise LW level, so increasing subtidal area and reducing intertidal area (in the absence of morphological response). No change in intertidal area can be predicted by the Emulator because of the constant uniform side-slope. The fixed side-slope also implies a significant increase of tidal prism for raised sea level (e.g. by 5 per cent for MSL+0.3m, and 15 per cent for MSL+1.0m in the Thames). In reality, such percentage increases are likely to be reduced by changed morphology. Similarly, Emulator baseline intertidal areas are liable differ from data (e.g. by a factor of 2 to 3 for the Thames, compare tables 4.1 and 3.1; the Emulator's baseline LW area is similar to other quoted values).

By dividing HW (or LW) volume by HW (or LW) area, a mean depth at HW (or LW) can be derived for baseline and future MSL scenarios. For the baseline, these derived mean depths for the Thames are 4.65m (HW), 1.72m (LW; mean tide). For MSL+0.3m, they are 4.80m (HW), 1.87m (LW). These increases by half the sea level rise are a direct result of the assumed triangular cross-section. The Emulator HW volume for the Thames is less than other estimates by a factor of 2-3; LW volume is smaller than other estimates by a factor five.

Flushing times vary from a few days to a few weeks (on the basis noted in Table 4.1). There is no correlation with estuary size as they depend also on tidal range and river flow. Infill times are much longer because they depend on the low concentration of transported sediment. Infill times increased in response to rising MSL, and shortened for increased mean river flow.

4.2 Hybrid Regime model

Results for the five estuaries on which the model was run are shown in table 4.2.

Table 4.2 Emulator and Hybrid Regime model results

Estuary	*Thames*	*Blackwater*	*Humber*	*Mersey*	*S'ton Water*
Scenario / characteristic					
MSL Baseline (2050) + ^{E}0.3m/^{E}1.0m					
Regime	634	110	1240	169	160
LW volume,	663/729	133/155	1290/1430	184/183	164/173
$10^6 m^3$ *Emulator*	124	51	330	106	130
	146/206	58/76	400/590	125/174	138/158
Regime	1340	330	3170	639	263
HW volume,	1390/1490	357/386	3270/3500	682/625??	268/281
$10^6 m^3$ *Emulator*	898	209	2510	1110	261
	957/1102	223/257	2700/3170	1170/1310	273/301
Regime	82	31.5	198	31.5	26.7
LW area,	85/93	35.5/38.3	202/212	34.9/36.3	27.5/29.5
km^2 *Emulator*	72	22.7	223	60	27.2
	78/92	24.2/27.8	246/299	65/77	28.0/30.0

HW area, km²	*Regime*	142	44.1	323	82.8	35.5
	Emulator	143/144 193 199/214	44.1/44.5 46.1 47.6/51.2	323/324 618 641/694	85.6/83.7 194 199/211	36.3/37.4 38.6 39.4/41.4
% change for 2% bigger tide						
LW/HW volume; area	*Regime*	1.6/1.5; 1.7/-0.7	4.5/3.0; 3.8/0.0	0/0; 0/1.3	0.5/3.4; 3.5/1.7	-1.9/-0.4; -1.5/0.8
	Emulator	-3.4/1.2; -1.7/0.6	-2.0/1.0; -0.9/0.6	-3.5/1.3; -1.8/0.6	-4.4/1.4; -2.2/0.7	-0.8/0.6; -0.4/0.3
% change for 20% more river flow						
LW/HW volume; area	*Regime*	0.2/0; 0.2/0	1.8/0.9; 2.2/0.0	0/0; 0/0	0/-0.1; 1.6/-0.1	-1.2/-1.5; -1.5/0.3
	Emulator	30/10.6; 14/5.2	24/11.5; 11.5/5.6	30.6/10.6; 14.3/5.1	34.6/10.1; 16.0/5.0	19.1/13.3; 9.1/6.4
% change for [F] Full scenario						
LW/HW volume; area	*Regime*	44/32; 32/3.5	44/18; 20/1.1	15/10; 7, 0.3	11.8/0.1; 11.8/-7.1	15/13; 15/7
	Emulator	112/40; 46/18	92/48; 38/22	137/46; 54/21	120/35.2; 48.2/16.3	51/36; 23/17

[E] Approached at 6 mm/y, 20 mm/y respectively in Hybrid Regime model.
[F] Full scenario means MSL + 1m, + extra 2 per cent tide range + extra 20 per cent river flow.

In response to raised MSL, figures 4.2.1 to 4.2.3 show future Thames Estuary morphologies predicted by the Hybrid Regime model. Table 5 presents changes to some variables for sea level rise of 6mm/yr or 0.18m by 2030 (0.3m by 2050). [Intertidal and channel areas are just slightly greater than TE2100 values (table 3.1), probably as a result of a slight difference in the extent of the modelled estuary used to compare areas and volumes].

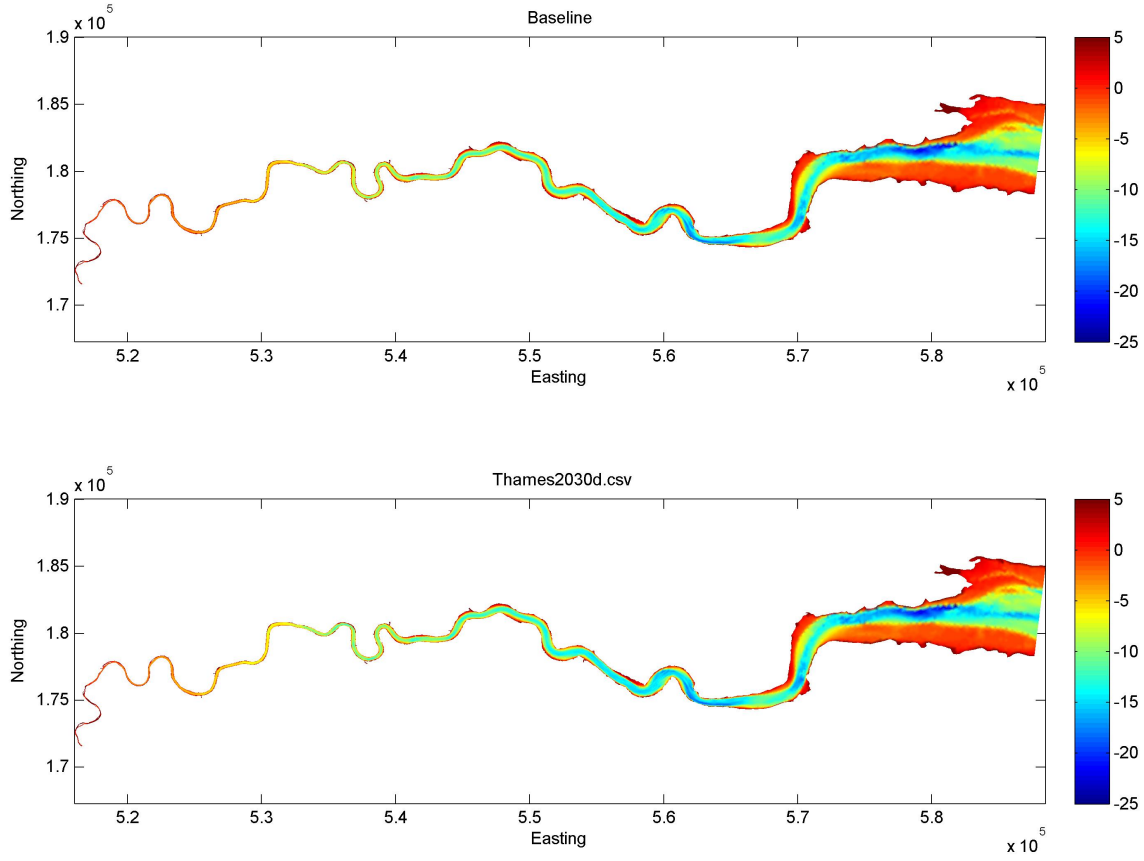

Figure 4.2.1 Hybrid Regime baseline and 2030 predictions (6mm/yr MSL rise).

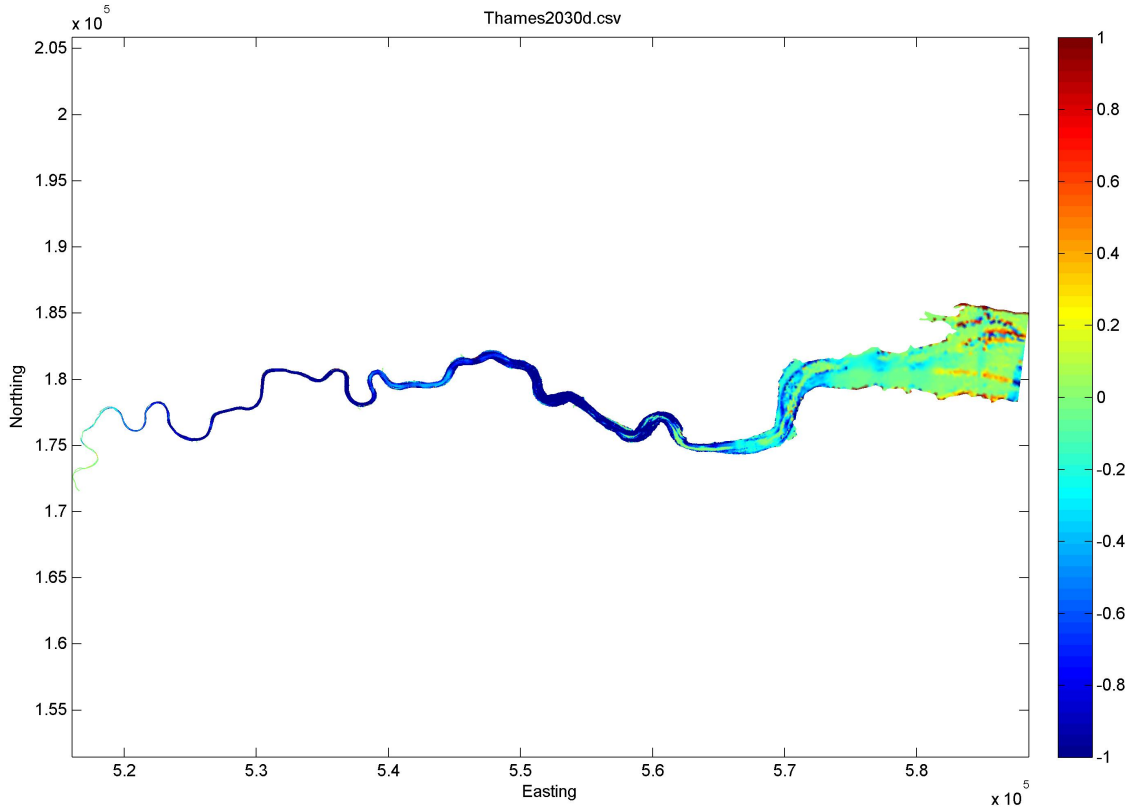

Figure 4.2.2 Hybrid-Regime predicted bathymetry changes to 2030 (6mm/yr MSL rise)

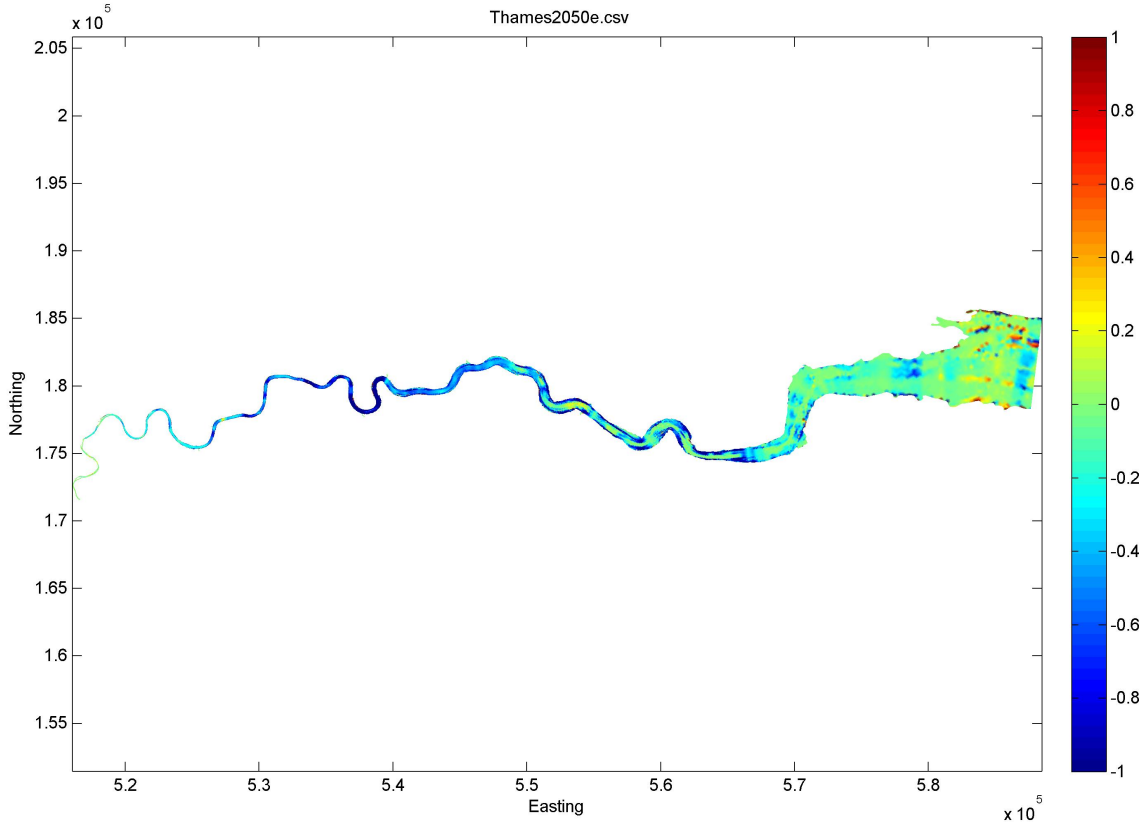

Figure 4.2.3 Hybrid-Regime predicted bathymetry changes, 2030-2050 (6mm/yr MSL rise)

The model's constrained HW area contributes to a predicted loss 4.8 km^2 of intertidal area after 0.18m of sea-level rise, contrasting with a TE2100-estimated loss 1.2 km^2 with no morphological response [and necessarily no change with the Emulator]. The Hybrid Regime model thus predicts erosion of the sea bed (through most of the estuary length) as well as deepening due to sea level rise. Average depth (derived as volume/area) is predicted to increase by 2030: by 0.5m at HW and by 0.22m at LW. [Emulator HW and LW depths necessarily increase by half the sea level rise]. Hence the Hybrid-Regime model predicts erosion of intertidal areas at many times the rate of sea level rise. This does not compare well with the HTA, Section 4.6. ??Predicted initial changes (figure 4.2.2; 2000-2030) are much greater than those later on (figure 4.2.3; 2030-2050).??

Hybrid-Regime and Emulator predictions of (percentage) increases in Blackwater volume for raised MSL are similar, despite LW volume discrepancies and no change of morphology in the Emulator. Respective Hybrid Regime, Emulator LW volume increases are 20 per cent, 15 per cent for the 0.3m sea level rise, 41 per cent, 49 per cent for the 1m sea level rise; HW volume increases are 8 per cent, 7 per cent for the 0.3m sea level rise, 17 per cent, 23 per cent for the 1m sea level rise.

For raised MSL in the Humber, the Hybrid Regime model increases (as percentages) are less than those predicted by the Emulator (probably excessive, especially as the Emulator LW baseline appears to be too small and rigid constraints on HW area are not allowed for). The Hybrid Regime model predicts increases ~ 15 per cent (LW volume), 10 per cent (HW volume), 7 per cent (tidal prism) per metre MSL rise (very close to Thames values). It predicts a 13 km^2 (10 per cent) loss of intertidal area after 1m of sea level rise.

For rising MSL in the Mersey, Hybrid Regime HW areas and volumes at first increase and then decrease; with eventual 1 m increased MSL, HW area is greater but volume is less (i.e. the mean depth is less). The Emulator LW volume is more sensitive to MSL rise, and HW area increase is greater than for the constrained Hybrid Regime model. These behaviours are considered unlikely, ??and as for the Thames the Hybrid Regime model prediction seems to evolve in response to the initial condition as well as sea level rise.??

For Southampton Water, the Emulator and Hybrid Regime model give comparable modest increases to HW and LW area if MSL rises. The Hybrid Regime results are intuitively correct here: intertidal area decreases with MSL rise ('coastal squeeze').

Thus "costal squeeze" attributable to constrained HW area is a prevalent outcome of the Hybrid Regime model for MSL rise.

For 2 per cent greater tidal range, changes predicted by the Hybrid Regime model and the Emulator are of order 2 per cent but qualitatively different (table 4.2). The Hybrid Regime model predicts an increase in LW area and volume except for Southampton Water (the Emulator necessarily predicts a decrease); the Blackwater has a predicted 7 per cent loss of intertidal area and large increase 3 per cent in HW depth. [For intertidal (HW-LW) area, the Emulator predicts an increase for increased tidal range, because it assumes a constant side slope]. Emulator & Hybrid-Regime results are comparable for Southampton Water (little change) and intuitively correct: intertidal area increases with increased tidal range.

On the other hand, Hybrid Regime predictions are relatively insensitive to increased river-flow. [The Emulator predicts a significant increase in estuary volumes]. For increased freshwater flow in Southampton Water, the Hybrid Regime model even predicts a decrease in HW and LW areas, and a small decrease of intertidal area; to maintain its regime state, the estuary widens and deepens to accommodate the extra flow.

4.3 "2.5-D"

In common with the Analytical Emulator, the "2.5-D" model has no morphological change for raised MSL. Thus the changes (necessarily increases) in HW and LW volumes and areas are broadly comparable between the two (table 4.3), depending only on their fixed geometries. Unlike the Dee and Ribble, the "2.5-D" model predicts an intertidal area decrease in the Mersey for raised MSL. Increased tide range likewise gives comparable changes (albeit per cent changes are sensitive to low baseline values, and LW volumes and areas necessarily decrease). Saltmarsh area (estimated as the area covered at Highest Astronomical Tide but uncovered at mean HW) notably decreases for raised MSL and increased tidal range. This is because the sides of the estuary are steeper above mean HW, consistent with the negative convexity (albeit this is evaluated between mean LW and mean HW).

Table 4.3 Emulator and "2.5-D" model results for the Mersey, Dee and Ribble.

Estuary ***Scenario / characteristic***	*Mersey*	*Dee*	*Ribble*
Baseline; 2050 MSL+0.3/ 1.0m			
LW volume, $10^6 m^3$ "2.5-D" *Emulator*	158; 166/185 106; 125/174	81; 88/106 733; 756/809	12; 14/21 5; 9/25
HW volume, $10^6 m^3$ "2.5-D" *Emulator*	510; 534/586 1110; 1170/1310	395; 421/489 1308; 1338/1409	195; 212/255 464; 501/591
LW area, km^2 "2.5-D" *Emulator*	28.1; 30.9/34.6 60; 65/77	22.0; 23.9/28.8 74.0; 75.1/77.7	9.08; 10.80/14.84 12.2; 16.8/22.6
HW area, km^2 "2.5-D" *Emulator*	66.8; 69.1/71.7 194; 199/211	75.3; 78.8/85.0 99; 100/102	49.1; 51.5/56.5 120; 124/135
2% bigger tide: % changes *LW/HW volume; area "2.5-D"* *Emulator*	-1/1.2; -1.4/0.6 -4.4/1.4; -2.2/0.7	-1.45/1.0; -0.87/0.86 -0.7/0.5; -0.3/0.3	-1.95/1.5; -1.8/1.0 -16.8/1.8; -8.8/0.9
River flow + 20%: % changes *LW/HW volume; area (Emulator)*	34.6/10.1; 16.0/5.0	18.4/13.7; 8.8/6.6	98/8.5; 41/4.2
"2.5-D" saltmarsh[S] Baseline, km^2 *% change: MSL +0.3/1.0m;* *tide+2%*	18.3 -12.4/-26.9; -2.3	50.8 -6.9/-23.0; -1.3	58.2 -4.1/-12.6; -0.85
"2.5-D" convexity[C]: Baseline *MSL +0.3/1.0m;* *tide+2%*	-0.107 -0.107/-0.134; -0.107	-0.075 -0.086/-0.113; -0.071	-0.130 -0.141/-0.173; -0.125
"2.5-D" mean SPM "in", *Baseline tonnes/tide* *% change: MSL+0.3/1.0m;* *tide+2%, wind 10m/s*	117000 0.7/6.1; 2.9, 0.7	24900 -8.4/-15; 8, 74	7120 14/55; 6.8, 102

[C]Cross-channel convexity meaning 0.5(MHW area + MLW area)/(Mean water level area) – 1 (identically zero for Analytical Emulator)

[S]*Saltmarsh is defined here as the area covered at Highest Astronomical Tide less that covered at mean HW.*

The mean (spring-neap) suspended sediment fluxes into these estuaries (table 4.3) all increase as expected with increased tidal range (and hence currents). However, trends with MSL vary and values for the Mersey are remarkably insensitive to wind-(wave) enhanced bed stress. Sediment deposited (per tide) in the Mersey and Dee is ~10 per cent of "flux in"; ~14 per cent in the Ribble. There is little change over the different scenarios in the Mersey and Ribble, but deposition in the Dee decreases markedly with increasing mean sea level.

4.4 ASMITA-type

ASMITA was applied to the Thames Estuary with initial volume and areas as in table 4.4a. Table 4.4b gives equilibrium coefficients for timescales 10s to 100s of years, selected as in Section 2.4. Table 4.4c gives the parameter values used for each element. The equilibrium concentration C_E at the outside-world boundary (0.000085) is measured concentration [O(50mg/l) at Southend] divided by typical Thames bed density (here taken as 600kg/m^3). The river concentration (C_R) available to the upper estuary section is 0.00014.

Table 4.4a Initial volume and area conditions used in ASMITA (From HRW, 2006a; Rossington and Spearman, 2007)

Section	Channel Area (x 10^6 m^3)	Flat Area (x 10^6 m^3)	Channel Volume (x 10^6 m^3)	Flat Volume (x 10^6 m^3)
Teddington to Broadness	17.8	6.1	102.8	13.7
Broadness to Lower Hope Point	19.8	6.2	153.6	14.6
Sea Reach	35.8	31.3	276.9	61.6

Table 4.4b Equilibrium parameters used in ASMITA

Section	a_f	a_c
Teddington to Broadness	0.11	0.88
Broadness to Lower Hope Point	0.11	0.60
Sea Reach	0.17	0.48

Table 4.4c Sediment exchange coefficients used in ASMITA. δ_{nm} is the coefficient for horizontal sediment exchange between elements n and m. (Subscripts f, c and o refer to the flats, channel and outside world.)

Section	Ws_n	D	δ_{fc}	D	δ_{cc} or δ_{co}
Teddington to Broadness	0.0006	125	15000	1200	260
Broadness to Lower Hope Point	0.0006	125	1350	4400	5000
Lower Hope Point to Southend	0.003	50	825	700	1270

The ASMITA model predicts a loss of intertidal area, 0.6 km^2 after 0.18m of sea level rise, compared with a TE2100-predicted loss of 0.9 km^2 with no morphological response and a TE2100-predicted gain of 0.8km^2 when both sea level rise and morphological change are taken into account. The HTA, however, extrapolates the current trend in sea level rise which is around 2mm/yr. For 2mm/yr MSL rise, ASMITA predicts 0.3 km^2 gain in intertidal area (Rossington and Spearman, 2007). ASMITA predicts a time-scale of 300 years for the estuary to reach dynamic equilibrium with sea level rising at 6 mm/yr.

4.5 Morpho-SandTrack

Figures 4.5.1 and 4.5.2 present Thames Estuary predictions from Morpho-SandTrack. These results have coarse resolution (c.f. Section 2.5); unfortunately too coarse to permit close comparison with observed trends (albeit sufficient to demonstrate the applicability of the

model). Landwards of Southend, visual comparison of Morpho-SandTrack and TE-2100 predictions (based on observed trends hitherto) does not conclusively lead to any areas of potential similarity. In the outer Thames Estuary, Morpho-Sandtrack predicts a relatively stable future system of channels and banks, except around the Edinburgh Channels crossing Long Sand. The TE2100 studies (HRW, 2005), concluded that the outer-estuary system of channels and banks appeared relatively stable (with extension of some of the banks seawards by up to a few km), except for the region around the Edinburgh Channels which appeared quite dynamic. Thus the model appears to represent the main features of the system.

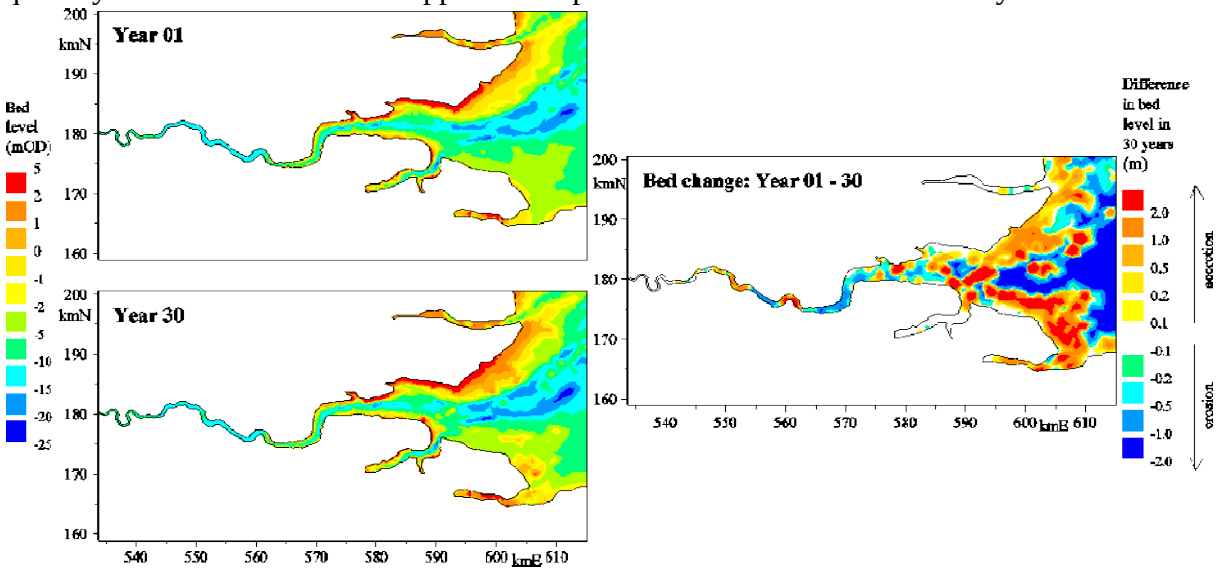

Figure 4.5.1 SandTrack model evolution of the Thames, year 1 to year 30 of a 50-year morphodynamic simulation, using yearly bed updates.

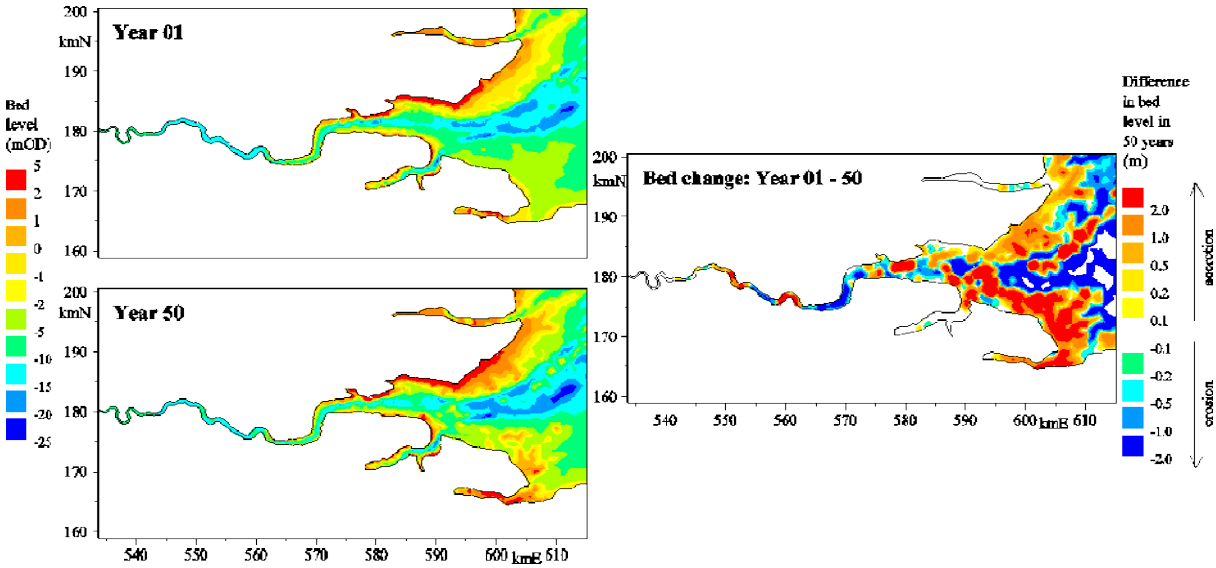

Figure 4.5.2 SandTrack model evolution of the Thames, year 1 to year 50 of a 50-year morphodynamic simulation, using yearly bed updates

4.6 TE2100 Historical Trend Analysis (HTA)

The two predicted 2030 geometries and differences (c.f. Section 2.6) are shown in figures 4.6.1 to 4.6.4 [the two geometries are the same in the omitted upstream area]. The predicted differences in bathymetry show several areas of continued accretion, deepening in some navigation channels and erosion of the subtidal foreshore between Putney and Richmond.

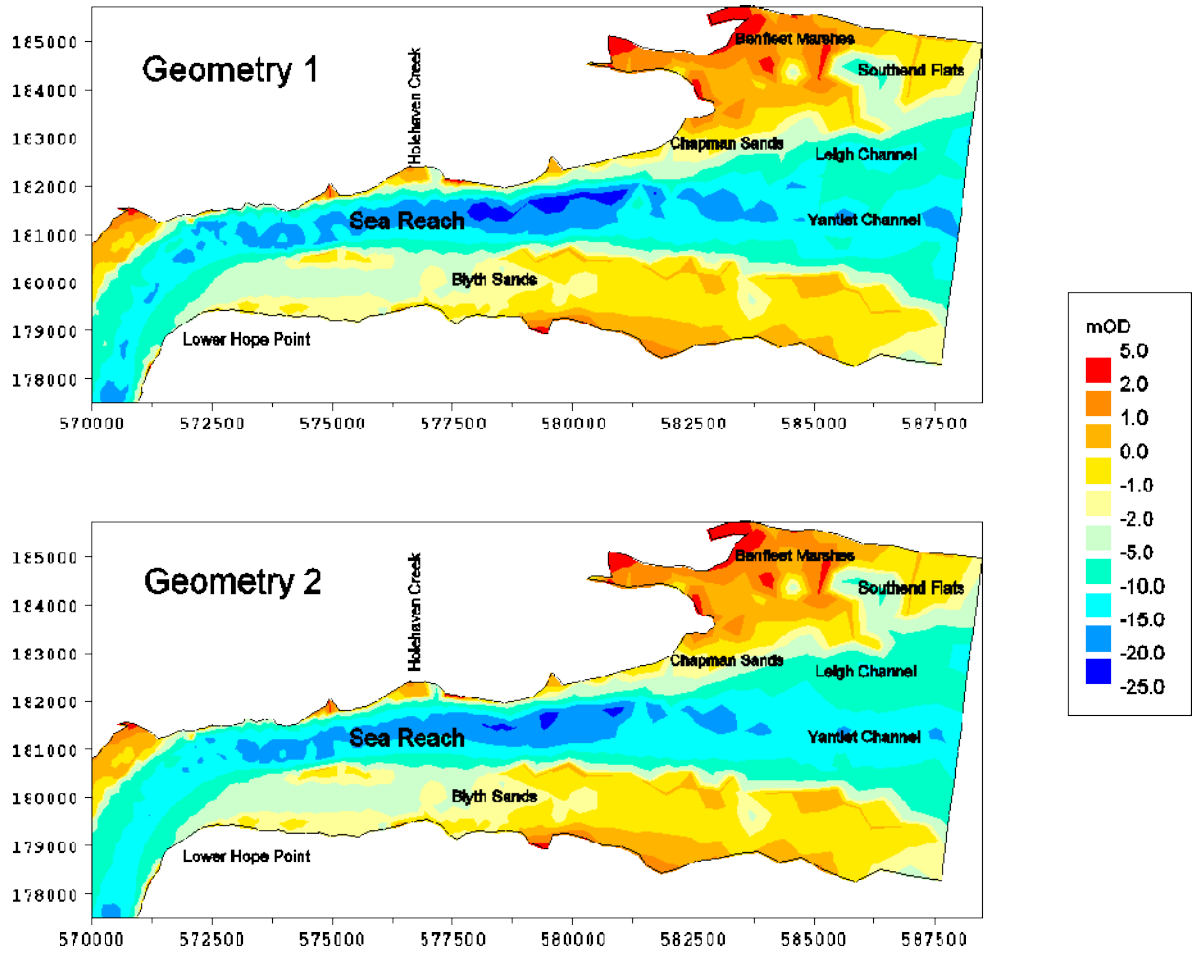

Figure 4.6.1 HTA-predicted 2030 bathymetry between Lower Hope Point and Southend

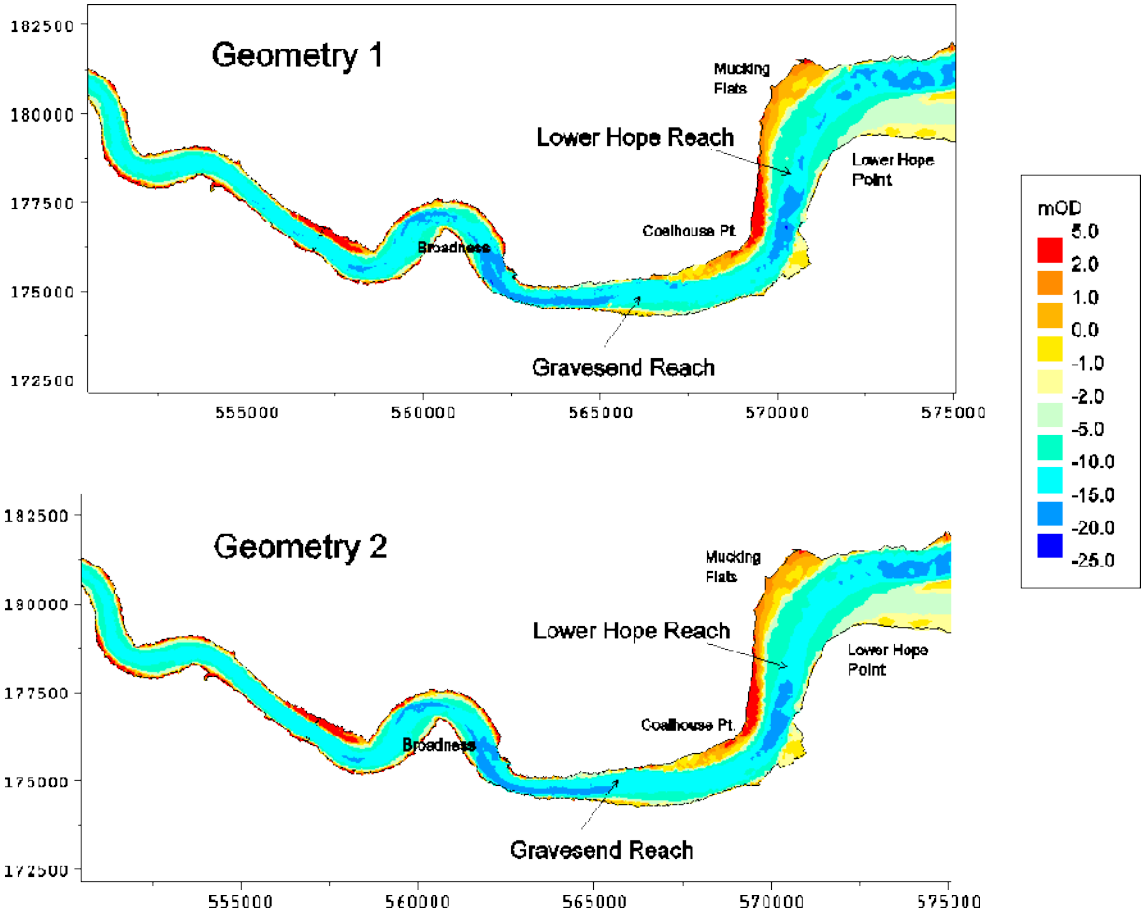

Figure 4.6.2 HTA-predicted 2030 bathymetry between Lower Hope Point and Erith

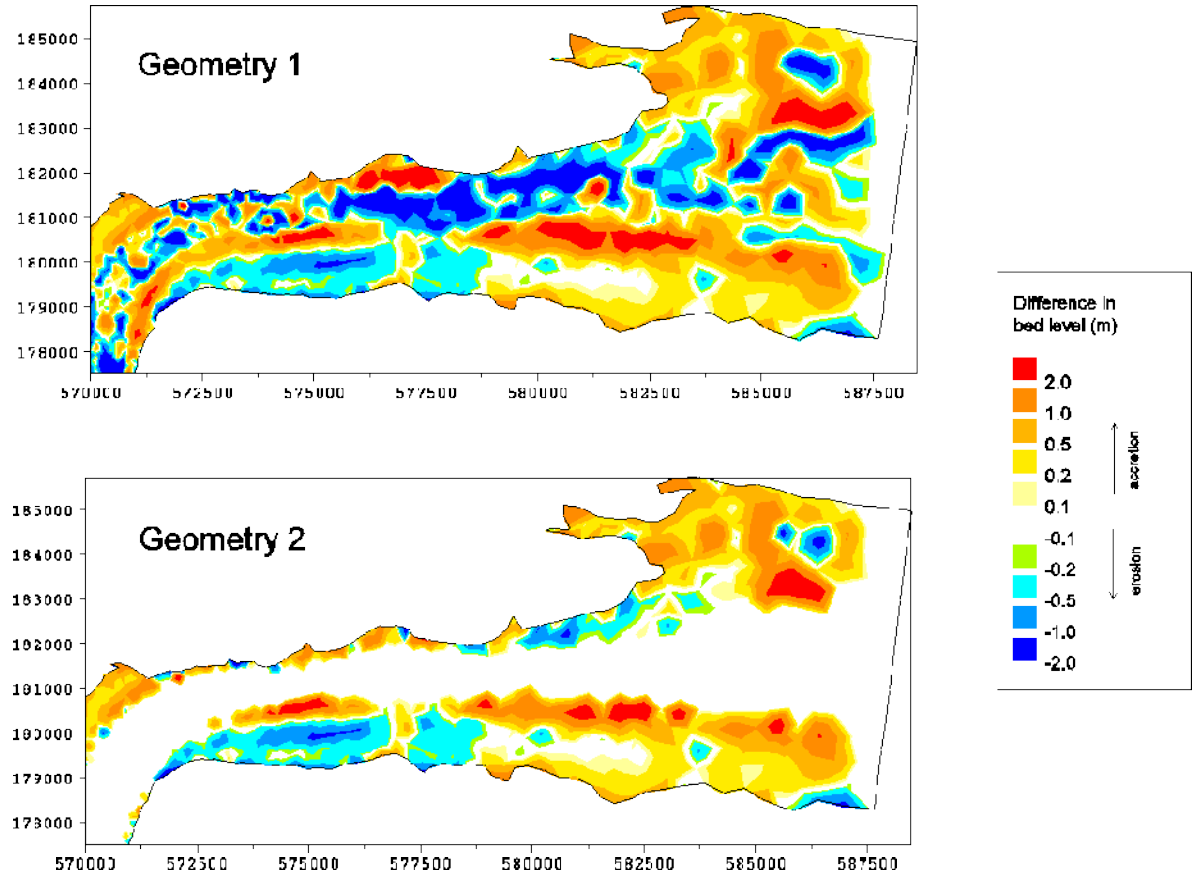

Figure 4.6.3 HTA-predicted bathymetry changes, 2000-2030, Lower Hope Point to Southend

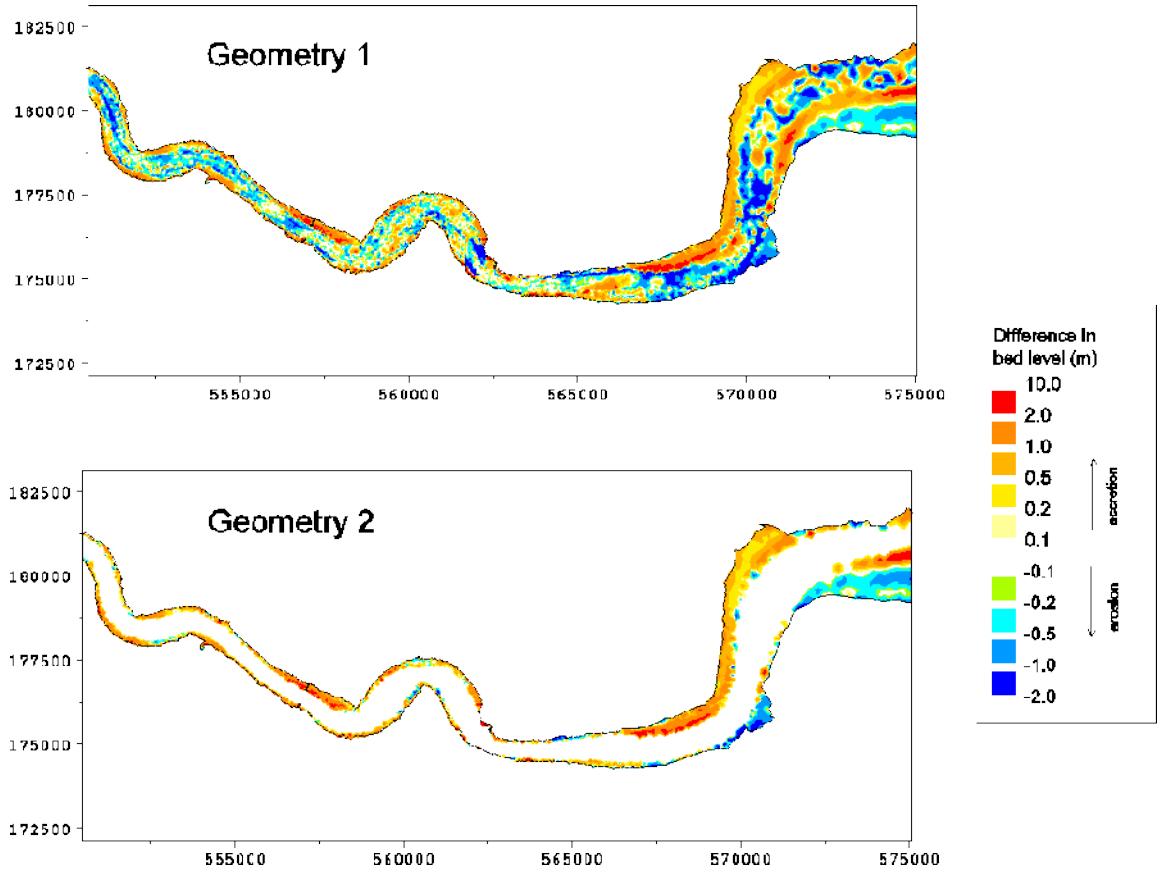

Figure 4.6.4 HTA-predicted bathymetry changes, 2000-2030, Erith to Lower Hope Point

Table 3.1 shows some estuary-wide volumetric comparisons with the 1920, 1970 and 2000 geometries. The volumes and areas shown are based on present mean sea level, *i.e.* the changes shown indicate changes in morphology only[1]. Table 3.1 shows a steady reduction in surface area of the Low Water channel (indicating a steady increase in intertidal area) and tidal volume in the Thames Estuary since 1920. The predicted 2030 geometries show this trend continuing.

4.7 Realignment model

This was applied to Tollesbury Creek (in the Blackwater) only. Figure 4.7.1 shows evolution of this managed realignment; the model's prediction compares reasonably with the observed evolution. This modelling is described in detail in Spearman (2007). For the longer term, the model predicts only slow development of (saltmarsh) area above HW neaps; vegetation-enhanced retention of deposited sediment tends to concentrate rather than extend saltmarsh development. Rising sea level (6 mm/yr) increases accretion in the model, but not enough to keep pace, so that salt marsh area decreases and the equilibrium volume of water increases by ~ 17 per cent in good agreement with ASMITA analysis.

[1] HW and LW volumes were calculated by calculating the maximum and minimum depths over the tide and summing over the whole estuary. HW (respectively LW) areas were calculated by summing up the areas over which the maximum (respectively minimum) depths are non zero.

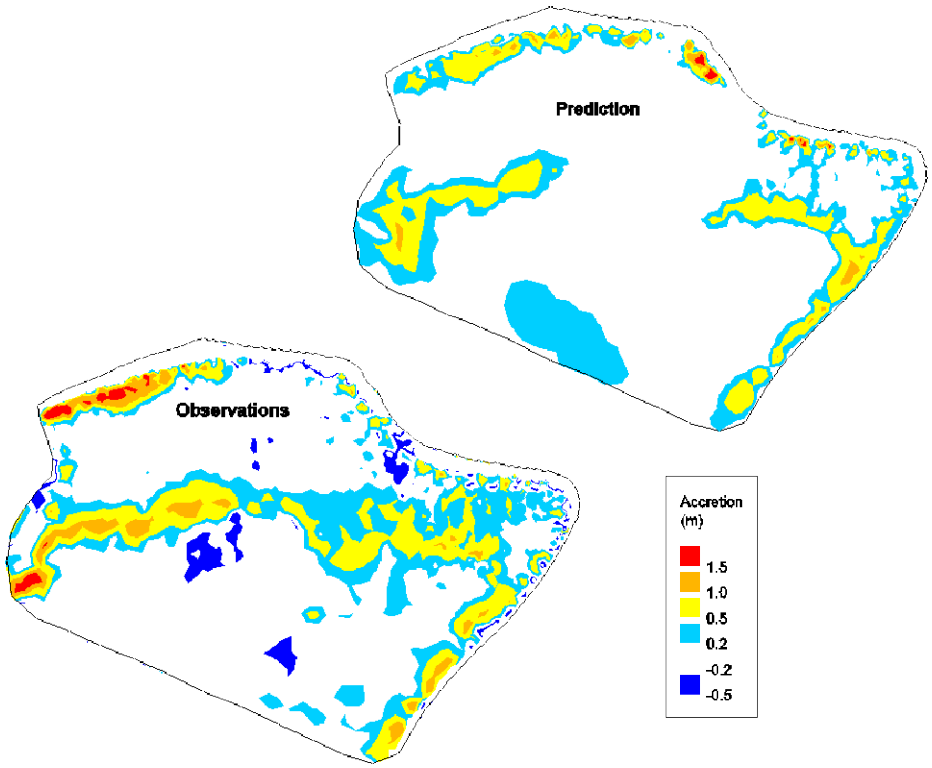

Figure 4.7.1 Comparison of observed and predicted bed level change in Tollesbury managed realignment site 1995-2002

4.8 Inverse model

This section presents results derived from the Inverse model as applied to the Humber (only). Bathymetry changes between each successive chart (figure 4.8.1) show the morphological changes of the estuary due to all external forcing. The reconstructed source functions, describing the morphological response of the estuary to non-diffusive processes, are shown for each survey interval (figure 4.8.2). Results of Empirical Orthogonal Functional analysis of the source function are then shown (figures 4.8.3, 4.8.4).

Figure 4.8.1 shows bathymetry changes in the outer and middle estuary between consecutive bathymetric surveys.

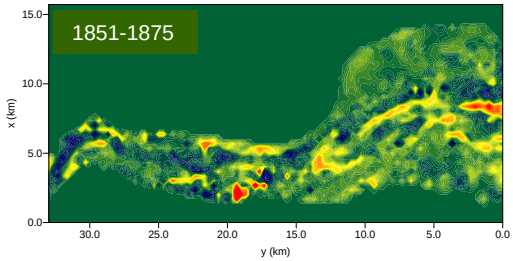
1851-1875
x (km)
y (km)

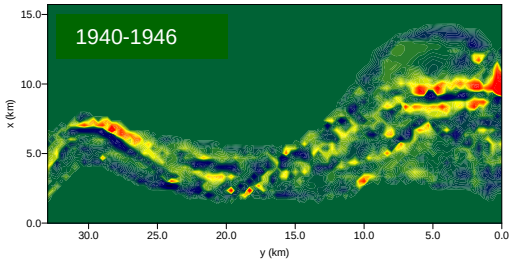
1940-1946
x (km)
y (km)

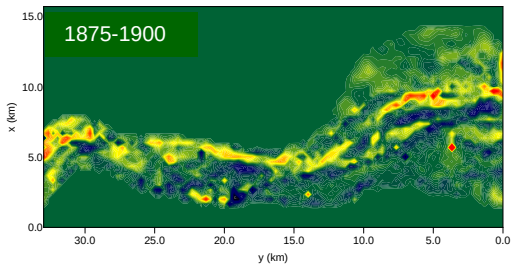
1875-1900
x (km)
y (km)

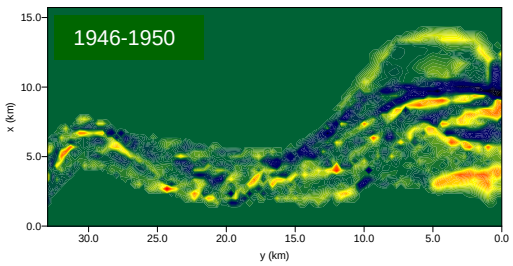
1946-1950
x (km)
y (km)

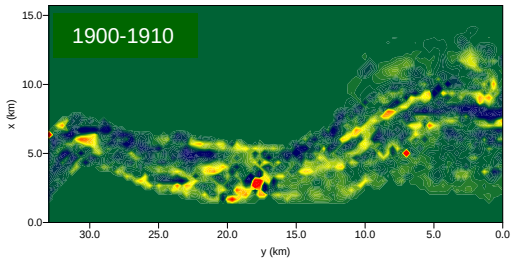
1900-1910
x (km)
y (km)

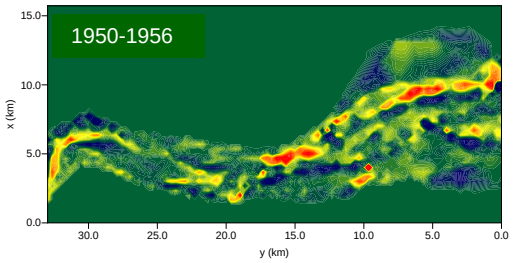
1950-1956
x (km)
y (km)

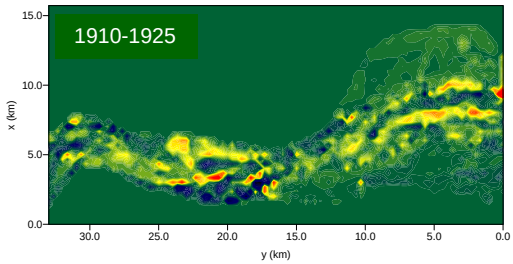
1910-1925
x (km)
y (km)

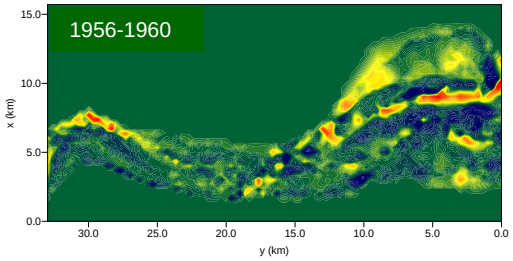
1956-1960
x (km)
y (km)

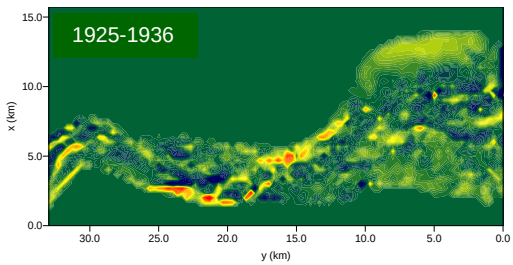
1925-1936
x (km)
y (km)

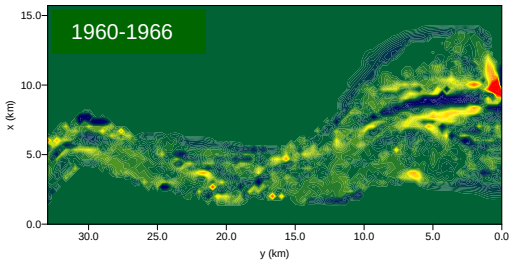
1960-1966
x (km)
y (km)

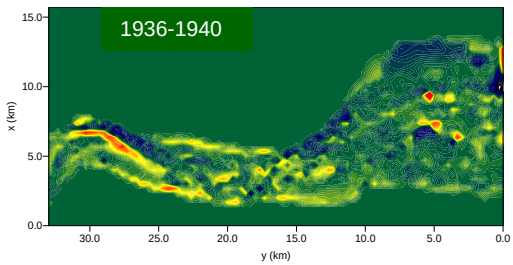
1936-1940
x (km)
y (km)

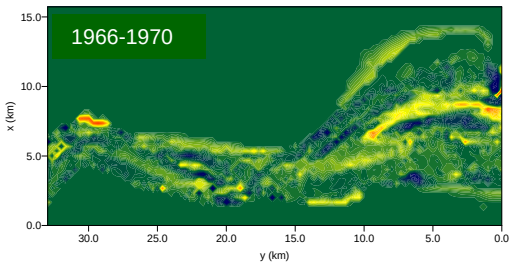
1966-1970
x (km)
y (km)

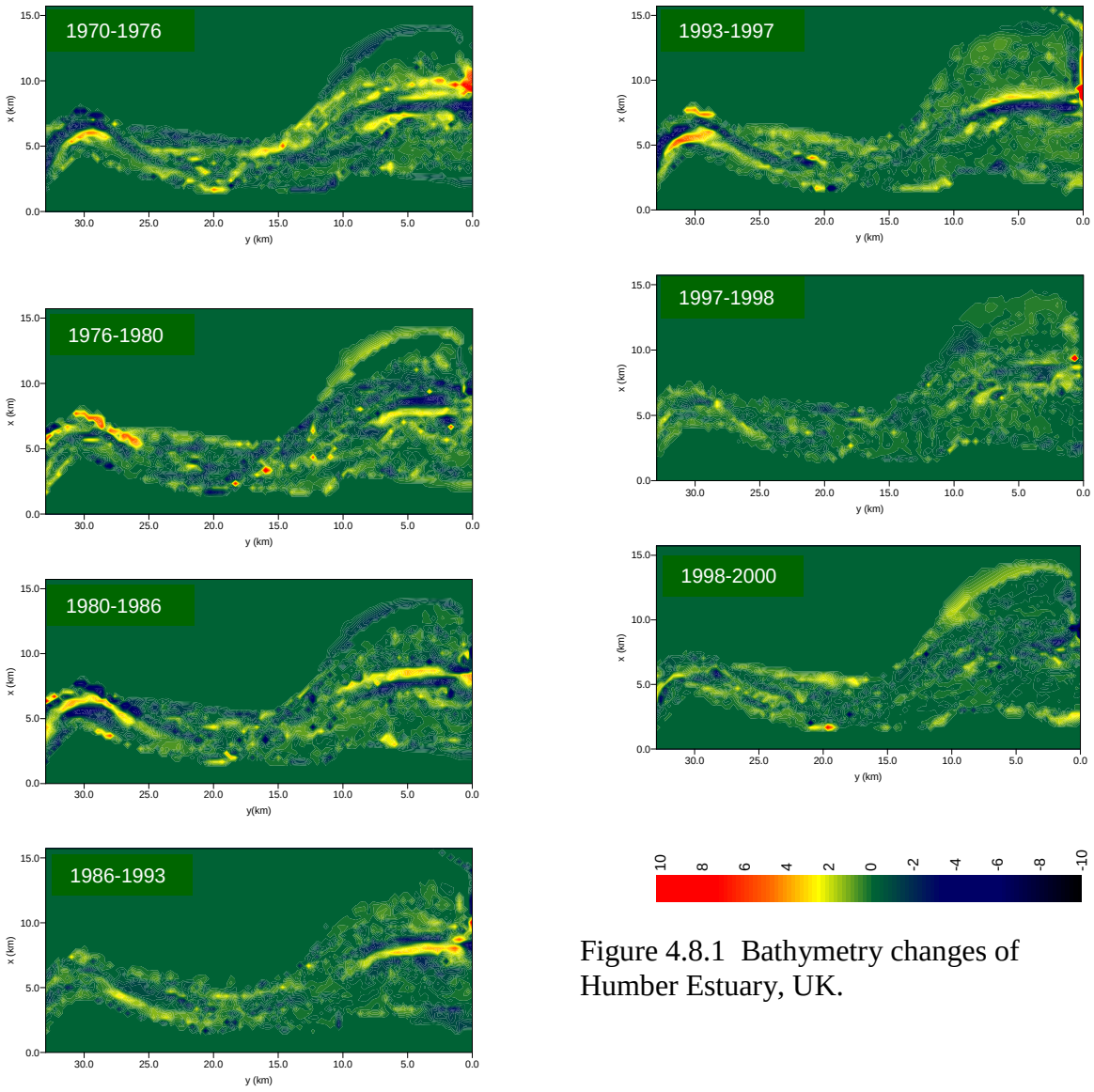

Figure 4.8.1 Bathymetry changes of Humber Estuary, UK.

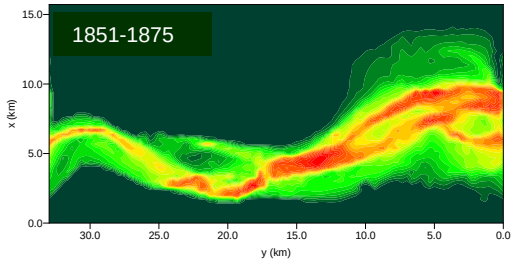
1851-1875
x (km)
y (km)

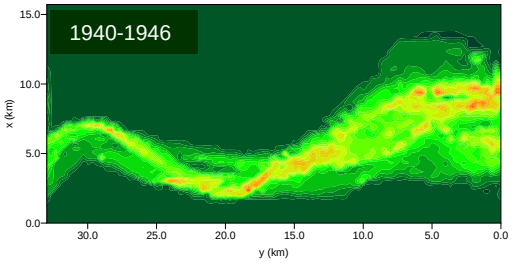
1940-1946
x (km)
y (km)

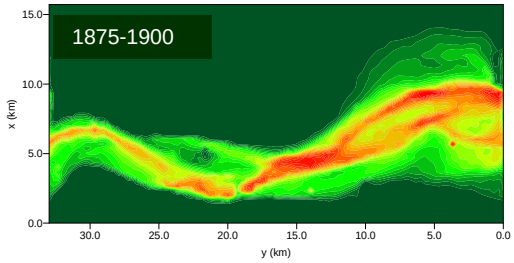
1875-1900
x (km)
y (km)

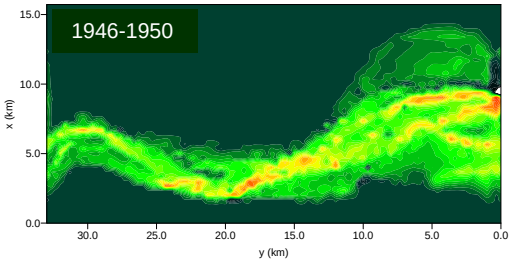
1946-1950
x (km)
y (km)

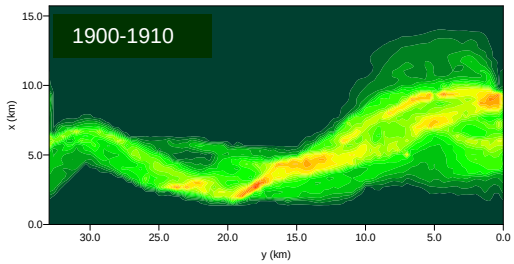
1900-1910
x (km)
y (km)

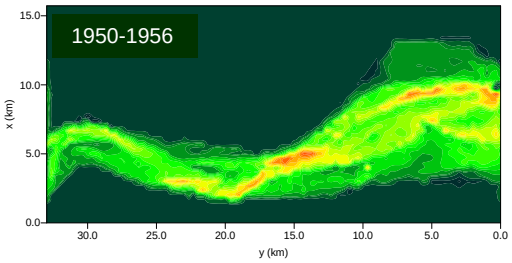
1950-1956
x (km)
y (km)

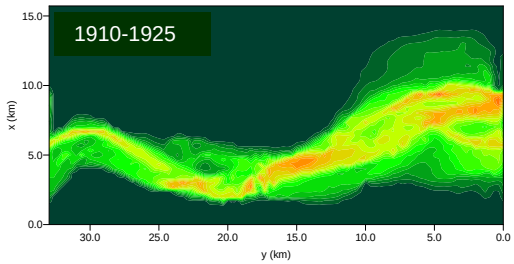
1910-1925
x (km)
y (km)

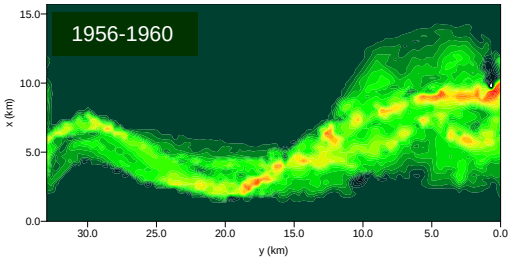
1956-1960
x (km)
y (km)

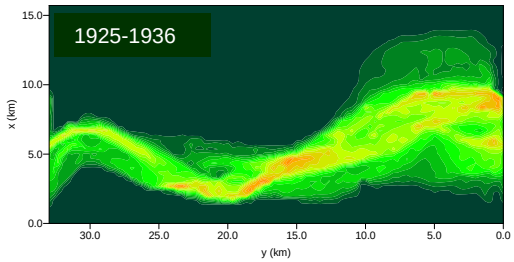
1925-1936
x (km)
y (km)

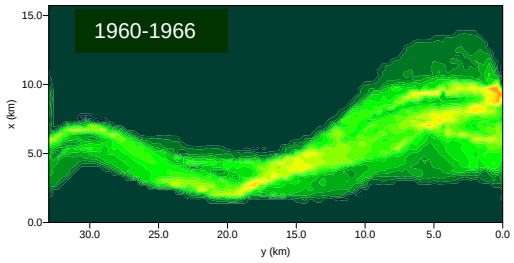
1960-1966
x (km)
y (km)

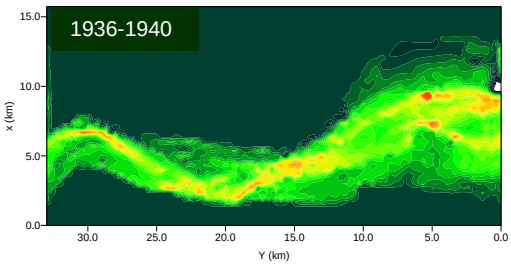
1936-1940
x (km)
Y (km)

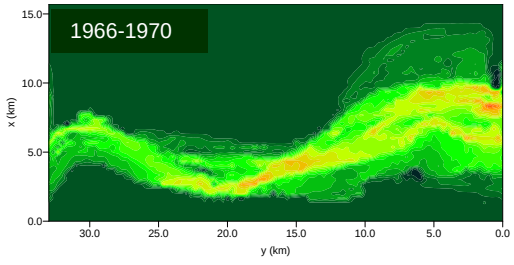
1966-1970
x (km)
y (km)

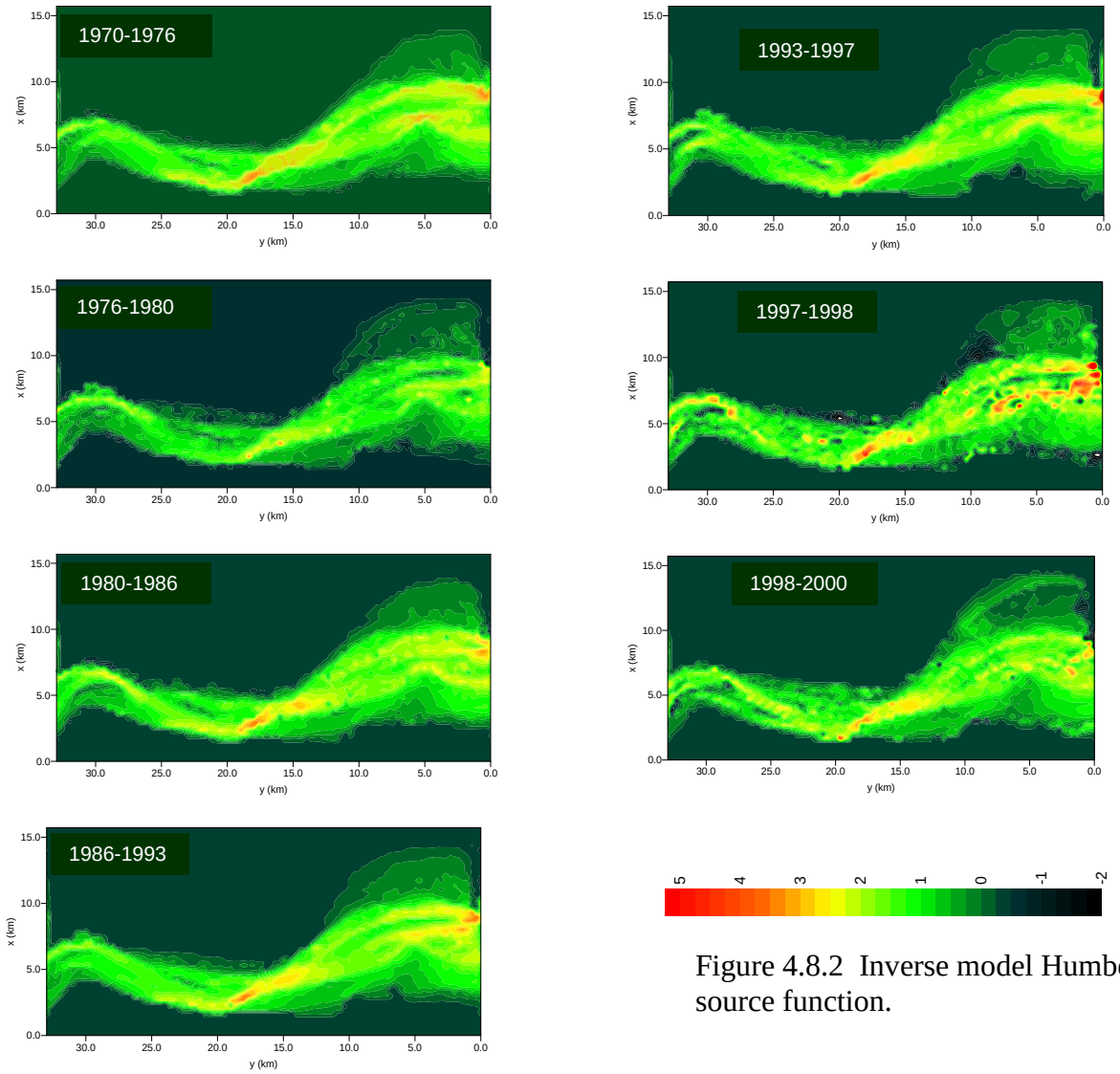

Figure 4.8.2 Inverse model Humber source function.

Inverse solutions were obtained using each pair of consecutive bathymetric surveys, to construct the source function corresponding to each survey interval (figure 4.8.2). Overall, there is no rapid variation of source function from one interval to another. Large scale features such as tidal channels, tidal flats and linear banks in the estuary are persistently visible. Smaller-scale structures are apparent than in bathymetric data *per se*. Other large-scale elongated features, possibly mud banks, are also visible in the middle estuary.

Table 4.8 Eigenvalues and variance of the first six eigenfunctions.

Eigenfunction	*Normalised Eigenvalue*	*% Variance*
1	0.923	-
2	0.014	18.1
3	0.013	16.8
4	0.009	12.3
5	0.008	10.7
6	0.006	7.4

Table 4.8 summarises the results of the EOF analysis (Section 2.8), and figure 4.8.3 shows plots of the 1st to 3rd spatial eigenfunctions. 92 per cent of the mean square data is contained in the first eigenfunction, which corresponds to the mean source function for the entire period considered. Second and subsequent eigenfunctions represent the variation of source function

about the mean; eigenfunctions 2 to 6 capture more than 65 per cent of this data variance. The second eigenfunction (shape of the strongest variation in the source function) shows areas of maxima and minima, mostly a few kilometres long, elongated along the estuary. The third eigenfunction shows smaller-scale spatial patterns.

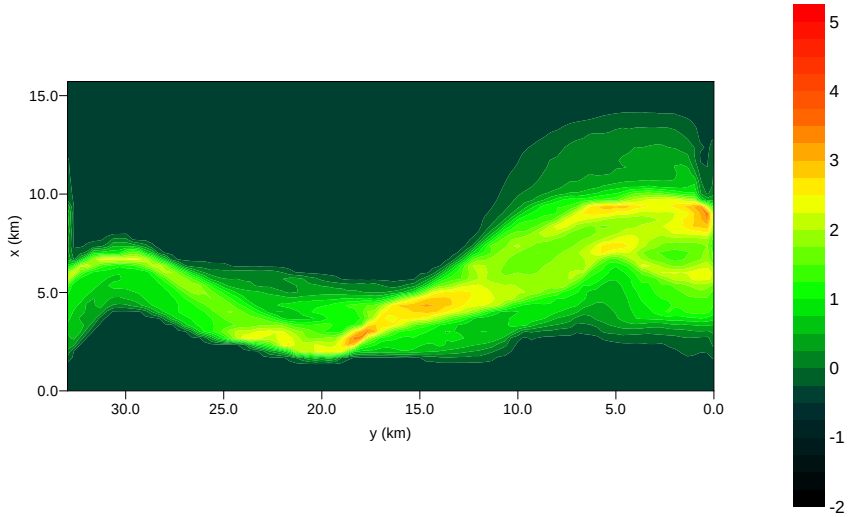

First spatial eigenfunction.

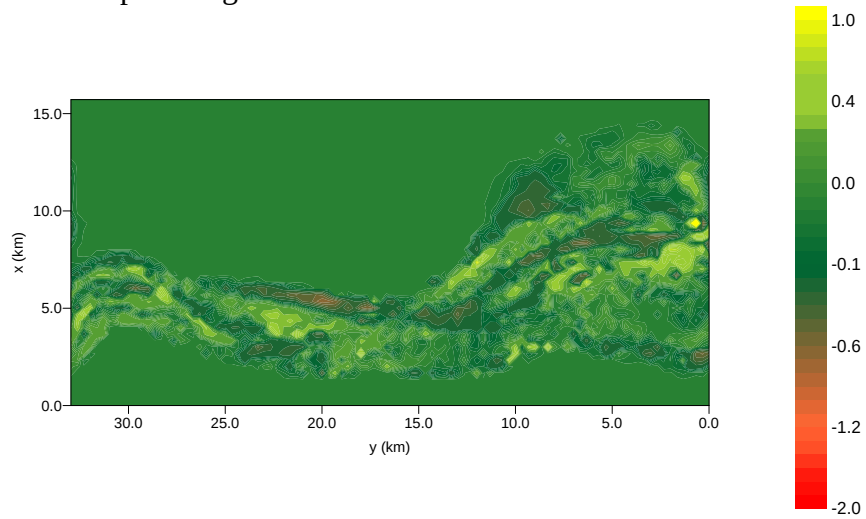

Second spatial eigenfunction.

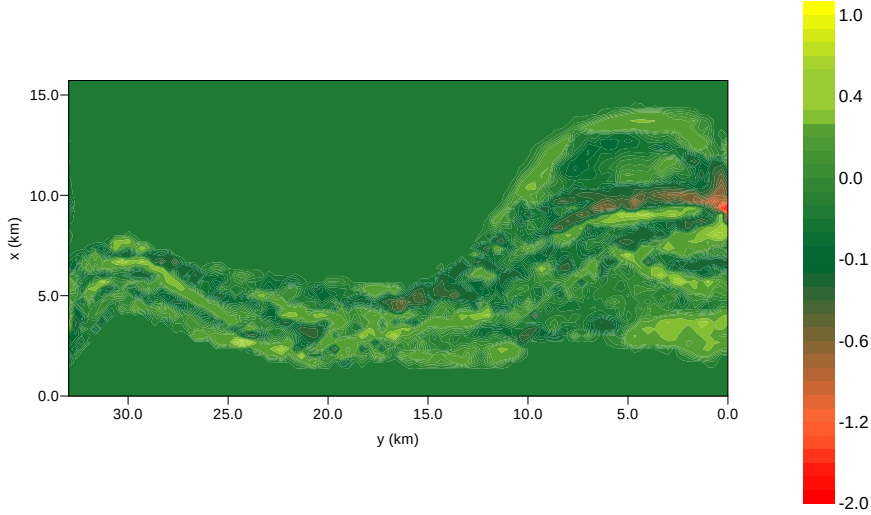

Third spatial eigenfunction.

Figure 4.8.3 Spatial orthogonal eigenfunctions for Inverse model Humber source function.

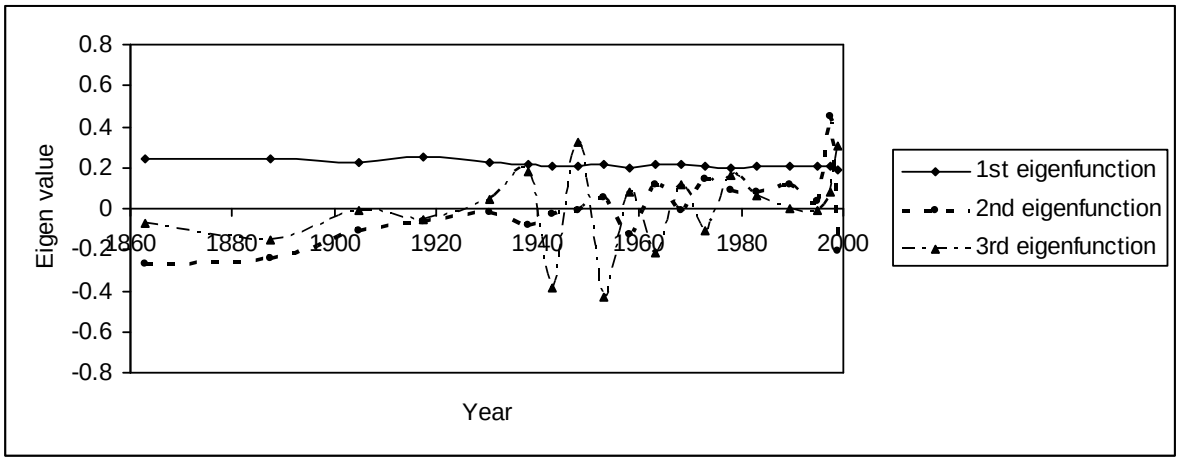

Figure 4.8.4 Temporal eigenfunctions for Inverse model Humber source function.

Temporal variation of the source eigenfunctions is shown in figure 4.8.4. The first function is almost constant; it corresponds to the temporal-mean source. The second function trends upwards, but has oscillations between 1960 and 1990; these may be attributed to bathymetry changes associated with large-scale dredging and development that took place at times between 1960 and 1994 (Townend and Whitehead, 2003). However, the survey frequency in general is not sufficient to a definite temporal signature of the second eigenfunction.

Direct comparison of the Inverse model results with those from the Emulator or the Hybrid Regime models is not possible; the outputs from the different models are different in type.

5. Discussion

The Thames including TE2100 studies (Table 3) has provided intercomparisons between the most models (Table 5). TE2100 studies predict changes to the geometry if there was just sea level rise (no morphological change), if there was just morphological change (no sea level rise) and for combined changes. These cases illustrate the possible range of outcomes.

Table 5 Emulator, Hybrid Regime, ASMITA and SandTrack comparison: Thames baseline; 2030 after 6 mm/yr; 2050 after 6 mm/yr

Model	*LW area (km^2)*	*HW area (km^2)*	*LW volume (km^3)*	*HW volume (km^3)*	*Suspended Sediment Fluxes (Tonnes / tide)*
Analytical Emulator	71.66; --; 77.89	193.25; --; 199.48	0.1235; --; 0.1459	0.90; --; 0.96	98,400; --; 103040
Hybrid Regime	85; 90.4; 93	140; 142; 142	0.663; 0.722; 0.752	1.31; 1.40; 1.44	N/A
ASMITA	73.8; 74.4 ; 74.7	117.7	--	--	--
SandTrack	75.7 to 83.9; 74.44 or 76.9; --	117.75; 117.75; --	0.5727; 0.5934; --	--	29,000 to 68,000; N/A; --

HW area increases by 2 km^2 in Hybrid Regime predictions, 6.2 km^2 in Emulator predictions (excessive) but does not increase significantly in the TE2100 prediction; HW intercepts tidal defences at most locations as reflected in constant ASMITA and SandTrack values. Tidal

defences also constrain the relatively small Hybrid Regime increase, which probably includes areas above current HW – e.g. saltmarsh around Canvey.

TE2100 suggests a small change in Thames LW area by 2030 compared with the Emulator and Hybrid Regime model predictions of 5-6 km^2 (5-10 per cent) increase. The TE2100 change in intertidal area (HW-LW area) in the range +/- 1 km^2 to 2030 (possibly much more longer-term) is likewise much less than the Hybrid-Regime-predicted decrease. Only ASMITA reproduced the current trend of intertidal area for the present ~2mm/yr rate of sea level rise.

The *Analytical Emulator* may not represent intertidal areas consistent with high and low water areas, and cannot represent loss of intertidal areas. It is also liable to represent channel volume and mean depths poorly (e.g. 1.7-4.8m compared with the more typical 8m for the Thames). Hence it is difficult to apply some aspects of the model responses meaningfully. These limitations and difficulties arise from the triangular cross-section, assumed for simplicity in the analysis underpinning the Emulator. In fact any fixed geometrical form could be used; alternatives could enable a better quantitative match to baseline areas and volumes. However, the present Emulator would require the geometrical form in the scenarios to be similar to the baseline form (only scale variations can be accommodated). There is no scope for constraint of HW area by fixed structures. Moreover, the only morphological change in these Emulator runs is the depth increase in response to increased river flow.

The *Hybrid Regime* model has many individual cross-sections and hence more flexibility to represent LW and HW areas and volumes accurately. Moreover, fixed surfaces can be defined to represent solid geology or structures where erosion is not allowed. Thus if HW area is constrained by sea defences, it will not increase under sea level rise in reality or in the model. However, initial response of the Hybrid Regime model to changed inputs was more than might be expected. This suggested that much predicted evolution was a response to the initial estuary condition (i.e. artificially caused by the model itself) rather than as a response to sea level rise. ??re-runs??

For greater sea level rise in the Thames, the Hybrid Regime model predicts more erosion. Its results contrast with infill as a result of sea level rise in ASMITA, where loss of intertidal area results only if sea level rises *faster* and infill lags behind. However, in other estuaries, Hybrid-Regime-predicted increases in volumes are no more than for the Emulator with no morphological change. Indeed, the Hybrid Regime model predicts shoaling of the Mersey at HW in the scenario of 1 m MSL rise over 50 years.

The *ASMITA* model provides intuitively correct results (loss of intertidal area if sea level rise outpaces infill); it was developed specifically to estimate morphological change under sea level rise. The model formulation is described by mathematical formulae, giving better *a priori* evaluation of the uncertainty inherent in the model prediction. Of the Emulator, Hybrid Regime and ASMITA models in the Thames, only ASMITA was validated against historical morphological change and simulated the current trend of increase in intertidal area.

The "*2.5-D*" model is able to represent LW and HW areas and volumes, limited only by the chosen resolution, to which flow in channels at LW is most sensitive. Differences from the Emulator arise from the latter's geometric limitation and possibly from differences of definition; differences from the Hybrid Regime model (in the Mersey) should be primarily due to definitions. "2.5-D" model results for changes under raised MSL and tidal range can

generally be interpreted in relation to the Emulator, because neither has morphological change. However, there are predictions of sediment transport and deposition (from which morphological change could be inferred until deposition patterns change significantly). These predictions enable inference of infill times to baseline HW level: respectively 152, 555, 685 years for the Mersey, Dee, Ribble. In practice deposition would change before infill is substantial, i.e. before the inferred infill time. These time-scales are comparable with those of the Emulator.

The present (*Morpho-)SandTrack* model is a research-level version, which could usefully be run for comparison purposes alongside more conventional Eulerian morphodynamic models, to gain experience of its relative performance (speed and results). It has some useful capabilities, and is complementary to the "2.5-D" model with Lagrangian transport. There were valuable exchanges of ideas and methodologies between the two models in the project. Both have their own individual niches in the overall modelling tool-kit.

The need to repeat flow model runs for 2-D morphology is not confined to Lagrangian morphological models such as Morpho-SandTrack; it holds more widely for B-U-based morphological modelling. Finer resolution than in SandTrack for the Thames is needed but demands much computer time. To address the issue, continuity might be used to alter current speeds for small bathymetric changes, so reducing the required number of flow model runs and making finer resolution feasible. However, such methods have yet to be proven.

Historical Trend Analysis (HTA) makes use of morphological change hitherto to guide expectations of future trends. However, as an empirical approach it should not be applied outside the range of experience. Hence it is not suited to estimates for scenarios of faster sea level rise, for which the ability of an estuary to "keep up" in the same way could be in doubt. As applied here, it was simply extrapolation of a present trend.

The *Inverse* model also makes use of morphological change hitherto, but with more reference to dynamics in the form of a diffusion-type equation to evolve the bed. In the Humber, source functions in tidal channels are positive, i.e. accretion is faster than diffusive as tidal channels draw sediment from surrounding mud flats and external sources (during the entire period). This is in line with ABPmer (2004): infilling of the estuary was observed during the last 150 years. However, the source functions differ from the corresponding bathymetry changes; the large-scale diffusive process is also significant in evolving estuary morphology.

Sensitivity of the source function to the diffusion coefficient was investigated by reconstructing the source function using coefficient values ± 50 per cent for several cases; there was no apparent change to the structure of the source function.

The Empirical Orthogonal Function analysis on the source function suggested strong spatial and temporal structure as a basis for prediction, dependent on no future intervention of unprecedented form. In practice, such application of the Inverse model appears to need bathymetry about every 10 years (this interval might have to be shorter for – e.g. small – estuaries with more rapid change). Unfortunately, few UK estuaries are completely surveyed this frequently; the Humber is our one example. On this basis it appears that the practical usefulness of the Inverse method is somewhat diminished.

Selection of the study area is important. Whereas the TE2100 study area included 42 km^2 of intertidal areas in the Thames Estuary (and the Hybrid Regime 57 km^2), the outer Thames

Estuary between the TE2100 boundary and a line from Margate to Clacton-on-Sea contains another 230 km^2 of intertidal area. Thus discrepancies between model predictions of estuary volume and area can arise from minor differences in definitions of the estuary limit.

Best practice when attempting to predict long-term changes in estuaries is to validate the model against historic change. Successful validation gives some confidence that the model predicts the key processes controlling morphological change, despite uncertainty inherent in the model prediction. Care is required when interpreting results from any individual model. Limitations of routines updating bed-morphology, and inherent unpredictability therein, can produce questionable results. Model results should ideally be compared with alternative techniques, to help establish the validity of predicted future morphologies. If validation data are lacking, generation of an ensemble of possible outcomes is likely to become best practice for such predictions. Importantly, predicted morphological trends should be consistent (in a broad sense) with the results of bottom-up models.

6. Conclusions and scope for future work

Of the models applied to the Thames, only ASMITA suggested that Thames infill keeps up with sea-level rise, in accord with the findings of HTA.

The Emulator struggles to represent intertidal areas consistent with high and low water areas. It cannot model loss of intertidal areas or constraints on high-water area by fixed structures. To enable the Emulator to represent HW and LW (hence intertidal) areas and volumes, the assumption of a triangular cross-section with uniform side-slope could be relaxed to some other uniform shape of cross section. It might be feasible to investigate (e.g.) power-law dependence of breadth and depth on along-estuary distance, implying self-similar rather than congruent cross-sections.

The Hybrid Regime model can represent HW and LW areas and volumes, given sufficient resolution, and provides intuitively correct results: intertidal area decreases with sea-level rise ('coastal squeeze') and increases with increased tidal range. It is desirable and conceivable that the Hybrid Regime model be developed to give a rate for the morphological evolution. If sediment transport, flow-dependent erosion and deposition were added to the underlying 1-D hydrodynamic model, a rate of change of area for each cross-section would be predicted. Work in FD2116 has already set out how the Hybrid Regime model could give a rate for morphological evolution and has shown how regime theory is an approximation to sediment transport (HRW *et al*., 2006).

The "2.5-D" and SandTrack models can represent LW and HW areas and volumes, limited only by the chosen resolution. With particle tracking they predict sediment transport and deposition. The "2.5-D" model could be extended to predict morphological evolution using (a modified form of) the development of SandTrack to Morpho-SandTrack in the project. It is desirable and possible to add waves to Morpho-SandTrack; they are already in SandTrack. These models suffer from having to repeat flow model runs continually as bathymetry evolves; there is scope for developing robust methods of accelerating this calculation.

The possible influence of estuarine circulation could be investigated, adding a (formulaic) supplement to the calculated flow in the Hybrid Regime, "2.5-D" and SandTrack models, as already done for the Mersey "2.5-D" model.

The Lagrangian particle-tracking method of the "2.5-D" model is being implemented in the POL Coastal Ocean Modelling System POLCOMS, a fully 3-D model with density effects (e.g. estuarine circulation is naturally modelled, given fresh river inflow).

ASMITA provides intuitively correct results (loss of intertidal area if sea level rises faster and infill lags behind); it appears to represent Thames evolution well. The project's extension of ASMITA to predict changes of element areas (as well as volumes) should be fully validated.

There is scope to develop the Realignment model to include effects of biology on bed shear stress, erosion of defences at the entrance to the set back site and erosion of the initial bed.

Historical Trend Analysis can guide expectations of future trends if applied within the range of experience. The Inverse model also uses previous changes, with more reference to dynamics via a bed-evolution equation. Predictions depend on relatively frequent surveys. If the Inverse model is to be used for prediction, there should be some hindcast tests (against some past data not used in the EOF analysis of Section 4.8) and trials for other estuaries.

If data are lacking for validation against historic change, then generation of an ensemble of possible outcomes is recommended, to test model results against alternatives and validate predicted future morphologies.

Estuaries do not all respond in the same way. This puts an onus on modelling the particular estuary studied.

References

ABPmer, 2004. Historical Analysis of Humber Estuary Morphology. ABPmer Report R.1005, October 2004.

Defra (2003). Climate change scenarios UKCIP02: implementation for flood and coastal defence. R&D Technical Summary W5B-029/TS and project W5B-029 outputs cited therein.

Defra (2006). Development and Flood Risk. Planning Policy Statement 25.

Di Silvio G (1989) Modelling the morphological evolution of tidal lagoons and their equilibrium configurations, XXIII Congress of the IAHR, Ottawa, August 1989.

Di Silvio G and Gambolati G (1990) Two-dimensional model of the long-term morphological evolution of tidal lagoons, VIII International Conference on Computational Methods in Water Resources, Venice, Italy, June 11-15, 1990.

Dronkers, J., van Os, AG. and Leendertse, J.J. (1982) Predictive salinity modelling of the Oosterschelde with hydraulic and mathematical models, Delft Hydraulics Laboratory Publication Number 264, April 1982.

EA (2000). Humber Estuary shoreline management plan. Environment Agency.

Flather, R. A., T.F. Baker, P.L. Woodworth, J.M. Vassie & D.L. Blackman, 2001. Integrated effects of climate change on coastal extreme sea levels. O3.4.1-O3.4.12 in, Proceedings of the 36th DEFRA Conference of River and Coastal Engineers. Keele University: Department for Environment, Food & Rural Affairs, Flood Management Division.

Galappatti, R. and C.B. Vreugdenhil (1985). A depth-integrated model for suspended transport, Journal of Hydraulic Research, 23 (4), pp359-377.

Horrilo-Caraballo, J.M. and D.E. Reeve, 2002. Eigenfunction analysis of complex estuary morphology. In: Proceedings 5th International Conference on Hydroinformatics. Cardiff, IWA Publishing, pp. 777-784.

HRW (2005). Thames Estuary 2100, Morphological changes in the Thames Estuary: analysis of changes in offshore area seaward of Sea Reach. Technical Note EP6.3, June 2005.
HRW (2006a). Thames Estuary 2100, Morphological changes in the Thames Estuary: Historic Trend Analysis. Technical Note EP6.4, January 2006.
HRW (2006b). Thames Estuary 2100, Morphological changes in the Thames Estuary: Top-down modelling. Technical Note EP6.5, February 2006.
HRW (2006c). Thames Estuary 2100, Morphological changes in the Thames Estuary: High Level Options, Analysis of potential changes to intertidal areas under different future climate change scenarios. Technical Note DTR4085/01, November 2006.
HRW, 2006d. Thames Estuary 2100: A Hybrid morphological prediction. Technical note EP 6.7, May 2006.
HRW, ABPmer and Pethick J (2006) Review and formalisation of geomorphological concepts and approaches for estuaries, Final Report prepared by HR Wallingford, ABPmer and Professor J Pethick for the Defra and Environment Agency Joint Modelling and Risk Theme, Report No: FD2116/TR2, Defra, December 2006
IPCC, 2001. Climate Change 2001. Intergovernmental Panel on Climate Change, Third Assessment Report. http://www.ipcc.ch/
Krone, R.B. (1962). Flume studies of the transport of sediment in estuarial shoaling processes final report. Hydraulic Engineering and Sanitary Engineering Research Laboratory, University of California, Berkeley, USA.
Lane, A. and D. Prandle, 2006. Random-walk particle modelling for estimating bathymetric evolution of an estuary. Estuarine, Coastal and Shelf Science, 68, 175–187.
Langbein, W.B. 1963. The hydraulic geometry of a shallow estuary. Bulletin of Int Assoc Sci Hydrology, 8, 84-94.
Manning, A.J. (2007a). Morphological modelling scenario comparisons using the Analytical Emulator for WP2.7 FD2107. HR Wallingford Tech. Report (*in prep*).
Manning, A.J. (2007b). Enhanced UK Estuaries database: explanatory notes and metadata. HR Wallingford Tech. Report (*in prep*).
Murray, P. and Pethick, J.S., 1999. Humber Estuary Geomorphological Studies, Stage 2: Meander energetic model. Report for the Environment Agency, Leeds, University of Newcastle, Newcastle.
Partheniades E (1965) Erosion and deposition of cohesive soils, Proceedings of the American Society of Civil Engineers (ASCE), Volume 91 (HY1), pp105-139.
Prandle, D. (2004). How tides and rivers determine estuarine bathymetries. Progress in Oceanography, 61, 1-26.
Prandle, D. (2006). Dynamical controls on estuarine bathymetry: Assessment against UK database. Est. Coastal and Shelf Sci., 68, 282-288.
Prandle, D., Lane, A. and Manning, A.J., (2005). Estuaries are not so unique. *Geophysical Research Letters*, Vol. 32, doi:10.1029/2005GL024797.
Prandle, D., Lane, A. and Manning, A.J., (2006). New typologies for estuarine morphology. *Geomorphology*, 81, 309-315.
Reeve, D.E. and J.M. Horrillo-Caraballo, 2003. Analysis and prediction of complex estuary morphology. In: Proceedings of COPEDEC VI 2003. Sri Lanka. Paper 117, Ch 17, 14pp.
Rossington, K. and J.R. Spearman, 2007. Development of estuary morphological models - Application of ASMITA to the Thames Estuary. *Report TR 162. HR Wallingford, UK. June 2007.*
Spearman, J.R. (2007). Hybrid modelling of managed realignment. *Report TR 157. HR Wallingford, UK. June 2007.*
Soulsby, R.L. (1997). Dynamics of Marine Sands: a manual for practical applications. Telford, London, xxi + 249 pp.

Soulsby, R.L., C.T. Mead and M.J. Wood, 2007. Development of a Langrangian morphodynamic model for sandy estuaries and coasts. *Report TR 159. HR Wallingford, UK. July 2007*.

Stive, M.J.F., M. Capobianco, Z.B. Wang, P. Ruol and M.C. Buijsman, 1998. Morphodynamics of a tidal lagoon and adjacent coast. Pp. 397-407 in: *Physics of Estuaries and Coastal Seas*: 8th International Biennial Conference on Physics of Estuaries and Coastal Seas, 1996. Balkema, Rotterdam.

Townend, I. and P. Whitehead, 2003. A preliminary net sediment budget for the Humber Estuary. The Science of the Total Environment, 314-316, 755-767.

UKCIP02: Hulme, M., G.J. Jenkins, X. Lu, J.R. Turnpenny, T.D. Mitchell, R.G. Jones, J. Lowe, J.M. Murphy, D. Hassell, P. Boorman, R. McDonald & S. Hill, 2002. Climate change scenarios for the United Kingdom: the UKCIP02 Scientific report.

Van Goor, M.A., T.J. Zitman, Z.B. Wang and M.J.F. Stive, 2003. Impact of sea-level rise on the morphological equilibrium state of tidal inlets. Marine Geology, 202, 211-227.

Wang, Z.B., 2005. Application of semi-empirical long-term morphological models ESTMORPH and ASMITA. *Z2839*, Delft Hydraulics, Delft.

Wright, A.P. and I.H. Townend (2006). Predicting intertidal change in estuaries. In: Proceedings of the 41st Defra Flood and Coastal Management Conference. Paper 04-3.

Young, I.R. and Verhagen, L.A. (1996). The growth of fetch limited waves in water of finite depth. Part 1. Total energy and peak frequency, Coastal Engineering, 29, 47-78.

Ergon House
Horseferry Road
London SW1P 2AL

www.defra.gov.uk